Statistical and Structural Approaches to Texture

ROBERT M. HARALICK, SENIOR MEMBER, IEEE

Abstract—**In this survey we review the image processing literature on the various approaches and models investigators have used for texture. These include statistical approaches of autocorrelation function, optical transforms, digital transforms, textural edgeness, structural element, gray tone cooccurrence, run lengths, and autoregressive models. We discuss and generalize some structural approaches to texture based on more complex primitives than gray tone. We conclude with some structural-statistical generalizations which apply the statistical techniques to the structural primitives.**

I. Introduction

TEXTURE is an important characteristic for the analysis of many types of images. It can be seen in all images from multispectral scanner images obtained from aircraft or satellite platforms (which the remote sensing community analyzes) to microscopic images of cell cultures or tissue samples (which the biomedical community analyzes). Despite its importance and ubiquity in image data, a formal approach or precise definition of texture does not exist. The texture discrimination techniques are, for the most part, *ad hoc*. In this paper, we survey, unify, and generalize some of the extraction techniques and models which investigators have been using to measure textural properties.

The image texture we consider is nonfigurative and cellular. We think of this kind of texture as an organized area phenomena. When it is decomposable, it has two basic dimensions on which it may be described. The first dimension is for describing the primitives out of which the image texture is composed, and the second dimension is for the description of the spatial dependence or interaction between the primitives of an image texture. The first dimension is concerned with tonal primitives or local properties, and the second dimension is concerned with the spatial organization of the tonal primitives.

Tonal primitives are regions with tonal properties. The tonal primitive can be described in terms such as the average tone, or maximum and minimum tone of its region. The region is a maximally connected set of pixels having a given tonal property. The tonal region can be evaluated in terms of its area and shape. The tonal primitive includes both its gray tone and tonal region properties.

An image texture is described by the number and types of its primitives and the spatial organization or layout of its primitives. The spatial organization may be random, may have a pairwise dependence of one primitive on a neighboring primitive, or may have a dependence of n primitives at a time. The dependence may be structural, probabilistic, or functional (like a linear dependence).

Image texture can be qualitatively evaluated as having one or more of the properties of fineness, coarseness, smoothness, granulation, randomness, lineation, or being motled, irregular, or hummocky. Each of these adjectives translates into some property of the tonal primitives and the spatial interaction between the tonal primitives. Unfortunately, few experiments have been done attempting to map semantic meaning into precise properties of tonal primitives and their spatial distributional properties.

To objectively use the tone and textural pattern elements, the concepts of tonal and textural feature must be explicitly defined. With an explicit definition, we discover that tone and texture are not independent concepts. They bear an inextricable relationship to one another very much like the relation between a particle and a wave. There really is nothing that is solely particle or soley wave. Whatever exists has both particle and wave properties and depending on the situation, the particle or wave properties may predominate. Similarly, in the image context, tone and texture are always there, although at times one property can dominate the other and we tend to speak of only tone or only texture. Hence, when we make an explicit definition of tone and texture, we are not defining two concepts: we are defining one tone-texture concept.

The basic interrelationships in the tone-texture concept are the following. When a small-area patch of an image has little variation of tonal primitives, the dominant property of that area is tone. When a small-area patch has wide variation of tonal primitives, the dominant property of that area is texture. Crucial in this distinction are the size of the small-area patch, the relative sizes and types of tonal primitives, and the number and placement or arrangement of the distinguishable primitives. As the number of distinguishable tonal primitives decreases, the tonal properties will predominate. In fact, when the small-area patch is only the size of one resolution cell, so that there is only one discrete feature, the only property present is simple gray tone. As the number of distinguishable tonal primitives increases within the small-area patch, the texture property will dominate. When the spatial pattern in the tonal primitives is random and the gray tone variation between primitives is wide, a fine texture results. As the spatial pattern becomes more definite and the tonal regions involve more and more resolution cells, a coarser texture results [64].

In summary, to characterize texture, we must characterize the tonal primitive properties as well as the spatial interrelationships between them. This implies that texture-tone is really a two-layered structure, the first layer having to do with specifying the local properties which manifest themselves in tonal primitives and the second layer having to do with specifying the organization among the tonal primitives. We, therefore, would expect that methods designed to characterize texture would have parts devoted to analyzing each of these aspects of texture. In the review of the work done to date, we will discover that each of the existing methods tends to

Manuscript received May 9, 1978; revised January 9, 1979. This work was supported by the U.S. Army under contract DAAK70-77-C-0156.

The author is with the Department of Electrical Engineering, Virginia Polytechnic Institute and State University, Blacksburg, VA 24061.

0018-9219/79/0500-0786$00.75

emphasize one or the other aspect and tends not to treat each aspect equally.

II. Review of the Literature on Texture Models

There have been eight statistical approaches to the measurement and characterization of image texture: autocorrelation functions, optical transforms, digital transforms, textural edgeness, structural elements, spatial gray tone cooccurrence probabilities, gray tone run lengths, and autoregressive models. An early review of some of these approaches is given by Hawkins [36]. The first three of these approaches are related in that they all measure spatial frequency directly or indirectly. Spatial frequency is related to texture because fine textures are rich in high spatial frequencies while coarse textures are rich in low spatial frequencies.

An alternative to viewing texture as spatial frequency distribution is to view texture as amount of edge per unit area. Coarse textures have a small number of edges per unit area. Fine textures have a high number of edges per unit area.

The structural element approach of Serra [78] and Matheron [49] uses a matching procedure to detect the spatial regularity of shapes called structural elements in a binary image. When the structural elements themselves are single resolution cells, the information provided by this approach is the autocorrelation function of the binary image. By using larger and more complex shapes, a more generalized autocorrelation can be computed.

The gray tone spatial dependence approach characterizes texture by the cooccurrence of its gray tones. Coarse textures are those for which the distribution changes only slightly with distance and fine textures are those for which the distribution changes rapidly with distance.

The gray level run length approach characterizes coarse textures as having many pixels in a constant gray tone run and fine textures as having few pixels in a constant gray tone run.

The autoregressive model is a way to use linear estimates of a pixel's gray tone given the gray tones in a neighborhood containing it in order to characterize texture. For coarse textures, the coefficients will all be similar. For fine textures, the coefficients will have wide variation.

The power of the spatial frequency approach to texture is the familiarity we have with these concepts. However, one of the inherent problems is in regard to gray tone calibration of the image. The procedures are not invariant under even a monotonic transformation of gray tone. To compensate for this, probability quantizing can be employed. But the price paid for the invariance of the quantized images under monotonic gray tone transformations is the resulting loss of gray tone precision in the quantized image. Weszka, Dyer, and Rosenfeld [92] compare the effectiveness of some of these techniques for terrain classification. They conclude that spatial frequency approaches perform significantly poorer than the other approaches.

The power of the structural element approach is that it emphasizes the shape aspects of the tonal primitives. Its weakness is that it can only do so for binary images.

The power of the cooccurrence approach is that it characterizes the spatial interrelationships of the gray tones in a textural pattern and can do so in a way that is invariant under monotonic gray tone transformations. Its weakness is that it does not capture the shape aspects of the tonal primitives. Hence, it is not likely to work well for textures composed of large-area primitives.

The power of the autoregression linear estimator approach is that it is easy to use the estimator in a mode which synthesizes textures from any initially given linear estimator. In this sense, the autoregressive approach is sufficient to capture everything about a texture. Its weakness is that the textures it can characterize are likely to consist mostly of microtextures.

A. The Autocorrelation Function and Texture

From one point of view, texture relates to the spatial size of the tonal primitives on an image. Tonal primitives of larger size are indicative of coarser textures; tonal primitives of smaller size are indicative of finer textures. The autocorrelation function is a feature which tells about the size of the tonal primitives.

We describe the autocorrelation function with the help of a thought experiment. Consider two image transparencies which are exact copies of one another. Overlay one transparency on top of the other and with a uniform source of light, measure the average light transmitted through the double transparency. Now, translate one transparency relative to the other and measure only the average light transmitted through the portion of the image where one transparency overlaps the other. A graph of these measurements as a function of the (x, y) translated positions and normalized with respect to the $(0, 0)$ translation depicts the two-dimensional autocorrelation function of the image transparency.

Let $I(u, v)$ denote the transmission of an image transparency at position (u, v). We assume that outside some bounded rectangular region $0 \leqslant u \leqslant L_x$ and $0 \leqslant v \leqslant L_y$ the image transmission is zero. Let (x, y) denote the x-translation and y-translation, respectively. The autocorrelation function for the image transparency d is formally defined by:

$$\rho(x, y) = \frac{1}{(L_x - |x|)(L_y - |y|)} \int_{-\infty}^{\infty} I(u, v) I(u + x, v + y)\, du\, dv \Big/ \frac{1}{L_x L_y} \int_{-\infty}^{\infty} I^2(u, v)\, du\, dv \qquad |x| < L_x \text{ and } |y| < L_y.$$

If the tonal primitives on the image are relatively large, then the autocorrelation will drop off slowly with distance. If the tonal primitives are small, then the autocorrelation will drop off quickly with distance. To the extent that the tonal primitives are spatially periodic, the autocorrelation function will drop off and rise again in a periodic manner. The relationship between the autocorrelation function and the power spectral density function is well known: they are Fourier transforms of one another [95].

The tonal primitive in the autocorrelation model is the gray tone. The spatial organization is characterized by the correlation coefficient which is a measure of the linear dependence one pixel has on another.

An experiment was carried out by Kaizer [41] to see if the autocorrelation function had any relationship to the texture which photointerpreters see in images. He used a series of seven aerial photographs of an Arctic region (see Fig. 1) and determined the autocorrelation function of the images with a spatial correlator which worked in a manner similar to the one envisioned in our thought experiment. Kaizer assumed the autocorrelation function was circularly symmetric and computed it only as a function of radial distance. Then for

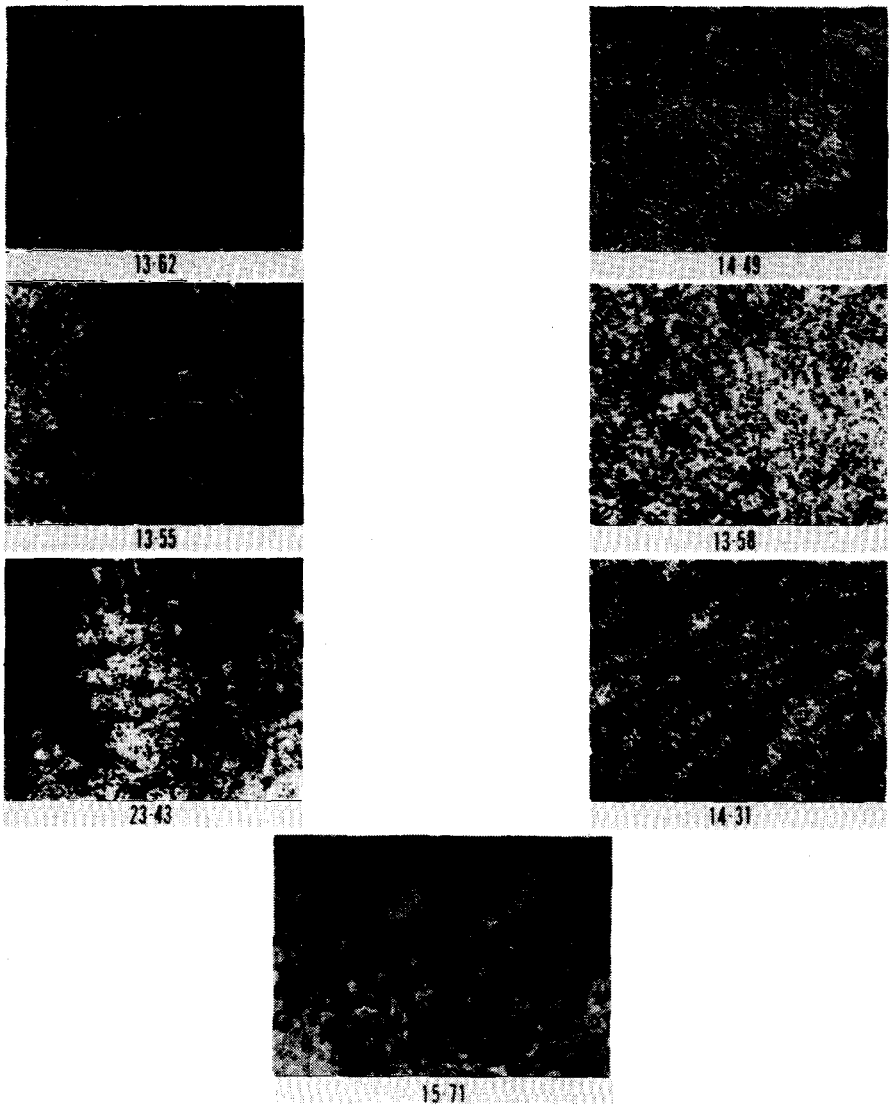

Fig. 1. Some of the image textures used by Kaizer in his autocorrelation experiment [41].

each image, he found the distance d such that the autocorrelation function ρ at d took the value $1/e$: $\rho(d) = 1/e$.

Kaizer then asked 20 subjects to rank the seven images on a scale from fine detail to coarse detail. He correlated the rankings with the distances corresponding to the $(1/e)$th value of the autocorrelation function. He found a correlation coefficient of 0.99. This established that at least for his data set; the autocorrelation function and the subjects were measuring the same kind of textural features.

Kaizer noticed, however, that even though there was a high degree of correlation between $\rho^{-1}(1/e)$ and subject rankings, some subjects put first what $\rho^{-1}(1/e)$ put fifth. Upon further investigation, he discovered that a relatively flat background (indicative of low frequency or coarse texture) can be interpreted as a fine textured or coarse textured area. This phenomena is not unusual and actually points out a fundamental characteristic of texture: it cannot be analyzed without a reference frame of tonal primitive being stated or implied. For any smooth gray-tone surface, there exists a scale such that when the surface is examined, it has no texture. Then as resolution increases, it takes on a fine texture and then a coarse texture. In Kaizer's situation, the resolution of his spatial correlator was not good enough to pick up the fine texture which some of his subjects did in an area which had a weak but fine texture.

B. Optical Processing Methods and Texture

Edward O'Neill's [61] article on spatial filtering introduced the engineering community to the fact that optical systems can perform filtering of the kind used in communication systems. In the case of the optical systems, however, the filtering is two-dimensional. The basis for the filtering capability of optical systems lies in the fact that the light amplitude distributions at the front and back focal planes of a lens are Fourier transforms of one another. The light distribution produced by the lens is more commonly known as the Fraunhofer diffraction pattern. Thus optical methods facilitate two-dimensional frequency analysis of images.

The paper by Cutrona *et al.* [12] provides a good review of optical processing methods for the interested reader. More recent books by Goodman [22], Preston [66], and Shulman [81] comprehensively survey the area.

In this section, we describe the experiments done by Lendaris and Stanley, and others using optical processing methods on

aerial or satellite imagery. Lendaris and Stanley [45], [46] illuminated small circular sections of low-altitude aerial photography and used the Fraunhofer diffraction pattern as features for identifying the sections. The circular sections represented a circular area on the ground of 750 ft. The major category distinction they were interested in making was man-made versus nonman-made. They further subdivided the man-made category into roads, road intersections, buildings, and orchards.

The pattern vectors they used from the diffraction pattern consisted of 40 components. Twenty components were averages of the energy in annular rings of the diffraction pattern and 20 were averages of the energy in 9° wedges of the diffraction pattern. They obtained over 90 percent identification accuracy.

Egbert *et al.* [17] used an optical processing system to examine the texture on LANDSAT imagery over Kansas. They used circular areas corresponding to a ground diameter of about 23 mi and looked at the diffraction patterns for the areas when they were snow covered and when they were not snow covered. They used a Recognition System diffraction pattern sampling unit having 32 sector wedges and 32 annular rings to sample and measure the diffraction patterns. They were able to interpret the resulting angular orientation graphs in terms of dominant drainage patterns and roads, but were not able to interpret the spatial frequency graphs which all seem to have had the same character: the higher the spatial frequency, the less the energy in that frequency band.

Honeywell Systems and Research Division has done work using optical processing on aerial images to identify species of trees. Using imagery obtained from Itasca State Park in northern Minnesota, photointerpreters identified five (mixture) species of trees on the basis of the texture: Upland Hardwoods, Jack pine overstory/Aspen understory, Aspen overstory/Upland Hardwoods understory, Red pine overstory/Aspen understory, and Aspen. They achieved classification accuracy of over 90 percent.

C. Digital Transform Methods and Texture

In the digital transform method of texture analysis, the digital image is typically divided into a set of nonoverlapping small square subimages. Suppose the size of the subimage is $n \times n$ resolution cells, then the n^2 gray tones in the subimage can be thought of as the n^2 components of an n^2-dimensional vector. The set of the subimages then constitutes a set of n^2-dimensional vectors. In the transform technique, each of these vectors is reexpressed in a new coordinate system. The Fourier transform uses the sine-cosine basis set. The Hadamard transform uses the Walsh function basis set, etc. The point to the transformation is that the basis vectors of the new coordinate system have an interpretation that relates to spatial frequency or sequency, and since frequency is a close relative of texture, such transformations can be useful.

The tonal primitive in spatial frequency (sequency) models is the gray tone. The spatial organization is characterized by the kind of linear dependence which measures projection lengths.

Gramenopoulos [23] used a transform technique employing the sine-cosine basis vectors (and implemented it with the FFT algorithm) on LANDSAT imagery. He was interested in the power of texture and spatial pattern to do terrain type recognition. He used subimages of 32 by 32 resolution cells and found that on a Phoenix, AZ, LANDSAT image 1049-17324-5, spatial frequencies larger than 3.5 cycles/km and smaller than 5.9 cycles/km contain most of the information needed to discriminate between terrain types. His terrain classes were: clouds, water, desert, farms, mountains, urban, riverbed, and cloud shadows. He achieved an overall identification accuracy of 87 percent.

Horning and Smith [37] have done work similar to Gramenopoulos, but with aerial multispectral scanner imagery instead of LANDSAT imagery.

Kirvida and Johnson [43] compared the fast Fourier, Hadamard, and Slant Transforms for textural features on LANDSAT imagery over Minnesota. They used 8×8 subimages and five categories: Hardwoods, Conifers, Open, City, Water. Using only spectral information, they obtained 74 percent correct identification accuracy. When they added textural information, they increased their identification accuracy to 99 percent. They found little difference between the different transform methods. (See also Kirvida [42].)

Maurer [51] obtained encouraging results classifying crops from low-altitude color photography on the basis of a one-dimensional Fourier series taken in a direction orthogonal to the rows.

Bajcsy and Lieberman [3], [4] divided the image into square windows and used the two-dimensional power spectrum of each window. They expressed the power spectrum in a polar coordinate system of radius r versus angle ϕ, treating the power spectrum as two independent one-dimensional functions of r and ϕ. Directional textures tend to have peaks in the power spectrum as a function of ϕ. Blob-like textures tend to have peaks in the power spectrum as a function of r. They showed that texture gradients can be measured by locating the trends of relative maxima of r or ϕ as a function of the position of the window whose power spectrum is being taken.

D. Textural Edgeness

The autocorrelation function, the optical transforms, and digital transforms basically all reference texture to spatial frequency. Rosenfeld and Troy [77] and Rosenfeld and Thurston [76] conceive of texture not in terms of spatial frequency but in terms of edgeness per unit area. An edge passing through a resolution cell can be detected by comparing the values for local properties obtained in pairs of nonoverlapping neighborhoods boardering the resolution cell. To detect microedges, small neighborhoods can be used. To detect macroedges, large neighborhoods can be used.

The local property which Rosenfeld and Thurston suggested was the quick Roberts gradient (the sum of the absolute value of the differences between diagonally opposite neighboring pixels). Thus a measure of texture for any subimage can be obtained by computing the Roberts gradient image for the subimage and from it determining the average value of the gradient in the subimage.

Sutton and Hall [83] extend Rosenfeld and Thurston's idea by making the gradient a function of the distance between the pixels. Thus for every distance d and subimage I defined over neighborhood N, they compute:

$$g(d) = \sum_{(i,j)\in N} \{|I(i,j) - I(I+d,j)| + |I(i,j) - I(i-d,j)| + |I(i,j) - I(i,j+d)| + |I(i,j) - I(i,j-d)|\}.$$

The curve of $g(d)$ is like the graph of the minus autocorrelation function translated vertically.

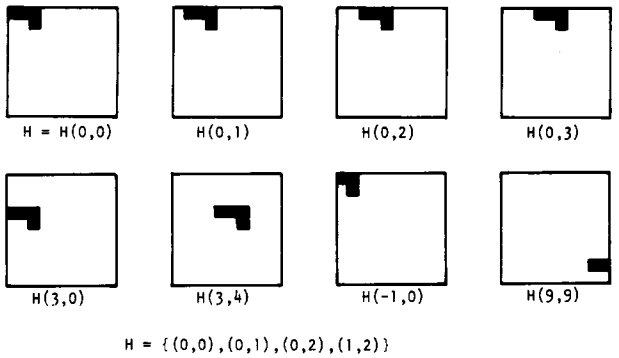

Fig. 2. Set H and some of its translates.

Sutton and Hall applied this textural measure in a pulmonary disease identification experiment and obtained identification accuracy in the 80 percentile range for discriminating between normal and abnormal lungs when using a 128 X 128 subimage.

Triendl [90] measures degree of edgeness by filtering the image with a 3 X 3 averaging filter and a 3 X 3 Laplacian filter. The two resulting filtered images are then smoothed with an 11 X 11 smoothing filter. The two values of average tone and roughness obtained from the low- and high-frequency filtered image can be used as textural features.

Hsu [38] determines textural edgeness by computing gradient-like measures for the gray tones in a neighborhood. If N denotes the set of resolution cells in a neighborhood about a pixel, and g_c is the gray tone of the center pixel, μ is the mean gray tone in the neighborhood, and ρ is a metric, then Hsu suggests that

$$\sum_{(i,j)\in N} \rho(I(i,j),\mu), \qquad \sum_{(i,j)\in N} \rho(I(i,j),g_c), \qquad \text{and } \rho(\mu,g_c)$$

are all appropriate measures for textural edgeness at a pixel.

E. Texture and Mathematical Morphology

A structural element and filtering approach to texture on binary images was proposed by Matheron [49] and Serra and Verchery [80]. Their basic idea is to define a structural element as a set of resolution cells constituting a specific shape such as a line or a square and to generate a new binary image by translating the structural element through the image and eroding by the structural element the figures formed by contiguous resolution cells having the value 1. The textural features can be obtained from the new binary image by counting the number of resolution cells having the value 1. The structural element approach of Serra and Matheron is the basis of the Leitz texture analyses [58], [59], [78]. The approach has found wide application in the quantitative analysis of microstructures in materials science and biology.

To make these ideas precise, we first define the translate of a set. Let Z be the set of integers $Z_r, Z_c \subseteq Z$ and $H \subseteq Z \times Z$. For any pair $(i,j) \in Z \times Z$, the translate $H(i,j)$ of H in the subset $Z_r \times Z_c$ is defined by:

$$H(i,j) = \{(m,n) \in Z_r \times Z_c | \text{ for some } (k,l) \in H, m = k+i \text{ and } n = l+j\}.$$

Fig. 2 illustrates a set and some of its translates.

Let $Z_r \times Z_c$ be the spatial domain of the given binary image I and F be that subset of resolution cells in $Z_r \times Z_c$ which take on the value 1 for image I. The erosion $F \ominus H$ of F by H is defined by:

$$F \ominus H = \{(m,n) \in Z \times Z | H(m,n) \subseteq F\}.$$

The eroded image J obtained by eroding I with structural element H is defined by:

$$J(i,j) = 1 \text{ if and only if } (i,j) \in F \ominus H.$$

The number of elements in the erosion $F \ominus H$ is proportional to the area of the binary 1 figures in the image. An interesting theoretical property of the erosion is that any operation which is antiextensive, increasing, and idempotent must be made up of erosions [44], [50], [79].

Textural properties can be obtained from the erosion process by appropriately parameterizing the structural element and determining the number of elements of the erosion as a function of the parameter. For example, in Fig. 3 we consider a series of structural elements each of two resolution cells in the same line and separated by distances of 0 through 19. The image in Fig. 3 is then eroded by each of these structural elements producing the eroded images of Fig. 3. In Fig. 4, we illustrate a graph showing the area of the erosion as a function of the distance separating the two resolution cells of the structural elements. A function such as that graphed in Fig. 4 is called the covariance function. Notice how it has relative maxima at distances which are multiples of about $5\frac{1}{3}$ resolution cells. This implies that in the horizontal direction there is a strong periodic component in the original image of about $5\frac{1}{3}$ resolution cells.

The generalized covariance function can use more complicated structural elements and summarizes the texture information in the image. If $H(d)$ is a structural element having two parts where d represents the distance between these two parts, the generalized covariance function k for a binary image I is defined as:

$$k(d) = \#F \ominus H(d), \quad \text{where } F = \{(i,j) | I(i,j) = 1\}.$$

For the case where the structural element consists of two resolution cells in the same line separated by distance d, the generalized covariance reduces to the autocovariance function for the image I. The generalized covariance function corresponding to more complicated kinds of structural elements, however, provides information not contained in the autocovariance function. Serra and Matheron show how the generalized covariance function can determine mean size of tonal features, mean free distance between tonal features, etc.

F. Spatial Gray-Tone Dependence: Cooccurrence

One aspect of texture is concerned with the spatial distribution and spatial dependence among the gray tones in a local area. Julesz [39] first used gray tone spatial dependence cooccurrence statistics in texture discrimination experiments. Darling and Joseph [13] used statistics obtained from the nearest neighbor gray tone transition matrix to measure this dependence for satellite images of clouds and was able to identify cloud types on the basis of their texture. Bartels *et al.* [5] and Weid *et al.* [93] used one-dimensional cooccurrence in a medical application. Rosenfeld and Troy [77] and Haralick [24] suggested two-dimensional spatial dependence of the gray tones in a cooccurrence matrix for each fixed distance and/or angular spatial relationship; Haralick *et al.* [28], [32] used statistics of this matrix as measures of texture in satellite imagery [30], [31], aerial, and microscopic imagery

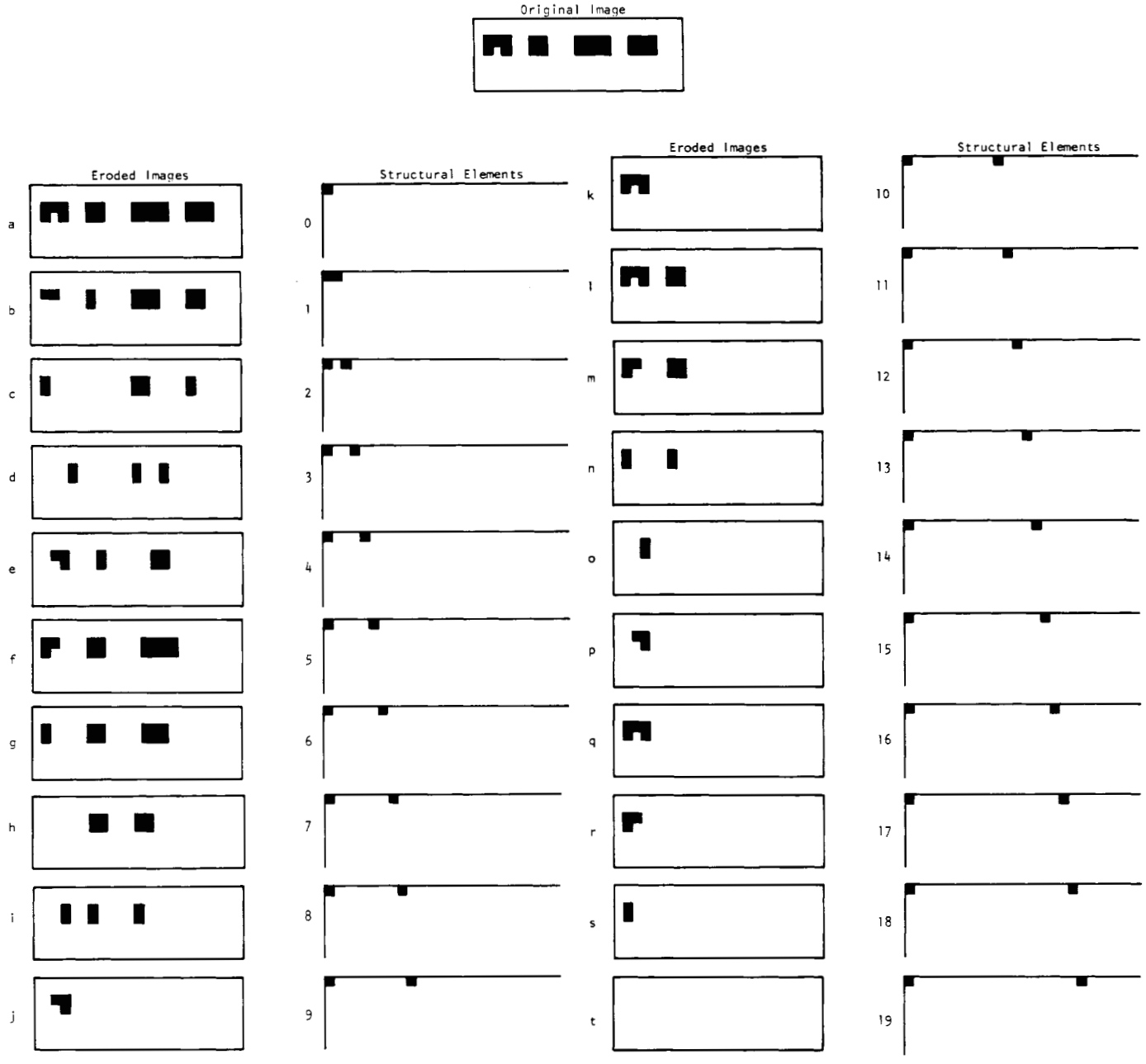

Fig. 3. The erosion operation for a number of different structural elements on the same image.

[30]. Chien and Fu [10] showed the application of gray tone cooccurrence to automated chest X-ray analysis. Pressman [65] showed the application to cervical cell discrimination. Chen and Pavlidis [9] used cooccurrence in conjunction with a split and merge procedure to segment an image on the basis of texture. All these studies achieved reasonable results on different textures using gray tone cooccurrence.

Suppose the area to be analyzed for texture is rectangular, and has N_c resolution cells in the horizontal direction, N_r resolution cells in the vertical direction, and that the gray tone appearing in each resolution cell is quantized to N_g levels. Let $L_c = \{1, 2, \cdots, N_c\}$ be the horizontal spatial domain, $L_r = \{1, 2, \cdots, N_r\}$ be the vertical spatial domain, and $G = \{1, 2, \cdots, N_g\}$ be the set of N_g quantized gray tones. The set $L_r \times L_c$ is the set of resolution cells of the image ordered by their row-column designations. The image I can be represented as a function which assigns some gray tone in G to each resolution cell or pair of coordinates in $L_r \times L_c$; $I: L_r \times L_c \rightarrow G$.

The gray tone cooccurrence can be specified in a matrix of relative frequencies P_{ij} with which two neighboring resolution cells separated by distance d occur on the image, one with gray tone i and the other with gray tone j. Such matrices of spatial gray tone dependence frequencies are symmetric and a function of the angular relationship between the neighboring resolution cells as well as a function of the distance between them. For a 0° angular relationship, they explicitly average the probability of a left-right transition of gray tone i to gray tone j within the right-left transition probability. Fig. 5 illustrates the set of all horizontal neighboring resolution cells separated by distance 1. This set, along with the image gray tones, would be used to calculate a distance 1 horizontal spatial gray tone dependence matrix.

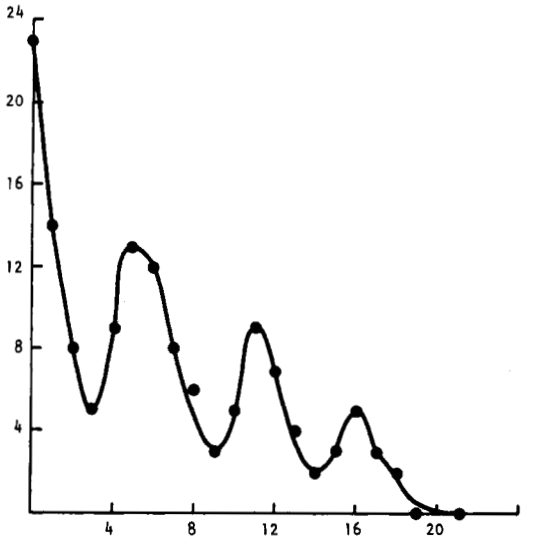

Fig. 4. The covariance function in the horizontal direction for the image of Fig. 3.

(1,1)	(1,2)	(1,3)	(1,4)
(2,1)	(2,2)	(2,3)	(2,4)
(3,1)	(3,2)	(3,3)	(3,4)
(4,1)	(4,2)	(4,3)	(4,4)

$L_y = \{1,2,3,4\}$

$L_x = \{1,2,3,4\}$

$$R_H = \{((k,l),(m,n)) \in (L_y \times L_x) \times (L_y \times L_x) \mid k-m=0,\ |l-n| = 1\}$$
$$= \{((1,1),(1,2)), ((1,2),(1,1)), ((1,2),(1,3)), ((1,3),(1,2)), ((1,3),(1,4)), ((1,4),(1,3)), ((2,1),(2,2)), ((2,2),(2,1)), ((2,2),(2,3)), ((2,3),(2,2)), ((2,3),(2,4)), ((2,4),(2,3)), ((3,1),(3,2)), ((3,2),(3,1)), ((3,2),(3,3)), ((3,3),(3,2)), ((3,3),(3,4)), ((3,4),(3,3)), ((4,1),(4,2)), ((4,2),(4,1)), ((4,2),(4,3)), ((4,3),(4,2)), ((4,3),(4,4)), ((4,4),(4,3))\}$$

Fig. 5. The set of all distance 1 horizontal neighboring resolution cells on a 4 × 4 image.

Formally, for angles quantized to 45° intervals, the unnormalized frequencies are defined by:

$$P(i,j,d,0^\circ) = \#\{((k,1),(m,n)) \in (L_r \times L_c) \times (L_r \times L_c) \mid k-m=0,\ |I-n| = d,\ \cdot I(k,1) = i,\ I(m,n) = j\}$$

$$P(i,j,d,45^\circ) = \#\{((k,1),(m,n)) \in (L_r \times L_c) \times (L_r \times L_c) \mid (k-m=d,\ I-n=-d) \text{ or } (k-m=-d,\ I-n=d),\ \cdot I(k,1) = i,\ I(m,n) = j\}$$

$$P(i,j,d,90^\circ) = \#\{((k,1),(m,n)) \in (L_r \times L_c) \times (L_r \times L_c) \mid |k-m| = d,\ I-n=0,\ \cdot I(k,1) = i,\ I(m,n) = j\}$$

$$P(i,j,d,135^\circ) = \#\{((k,1),(m,n)) \in (L_r \times L_c) \times (L_r \times L_c) \mid (k-m=d,\ I-n=d) \text{ or } (k-m=-d,\ l-n=-d),\ \cdot I(k,1) = i,\ I(m,n) = j\}$$

0	0	1	1
0	0	1	1
0	2	2	2
2	2	3	3

Grey Tone	0	1	2	3
0	#(0,0)	#(0,1)	#(0,2)	#(0,3)
1	#(1,0)	#(1,1)	#(1,2)	#(1,3)
2	#(2,0)	#(2,1)	#(2,2)	#(2,3)
3	#(3,0)	#(3,1)	#(3,2)	#(3,3)

F

$$0^\circ\ P_H = \begin{pmatrix} 4 & 2 & 1 & 0 \\ 2 & 4 & 0 & 0 \\ 1 & 0 & 6 & 1 \\ 0 & 0 & 1 & 2 \end{pmatrix} \qquad 90^\circ\ P_V = \begin{pmatrix} 6 & 0 & 2 & 0 \\ 0 & 4 & 2 & 0 \\ 2 & 2 & 2 & 2 \\ 0 & 0 & 2 & 0 \end{pmatrix}$$

$$135^\circ\ P_{LD} = \begin{pmatrix} 2 & 1 & 3 & 0 \\ 1 & 2 & 1 & 0 \\ 3 & 1 & 0 & 2 \\ 0 & 0 & 2 & 0 \end{pmatrix} \qquad 45^\circ\ P_{RD} = \begin{pmatrix} 4 & 1 & 0 & 0 \\ 1 & 2 & 2 & 0 \\ 0 & 2 & 4 & 1 \\ 0 & 0 & 1 & 0 \end{pmatrix}$$

Fig. 6. The spatial cooccurrence calculations [33].

Uniformity or energy (Related to the variance of $\{P_{11},\ldots,P_{ij},\ldots,P_{NN}\}$)	$\sum_{i,j} P_{ij}^2$
Entropy	$\sum_{i,j} P_{ij} \log P_{ij}$
Maximum probability	$\max_{ij} P_{ij}$
Contrast	$\sum_{i,j} \lvert i-j\rvert^k (P_{ij})^t$
Inverse difference moment	$\sum_{\substack{i,j \\ i \neq j}} \frac{(P_{ij})^t}{\lvert i-j\rvert^k}$
Correlation	$\sum_{i,j} \frac{(i-u)(j-u)P_{ij}}{\sigma^2}$
Probability of a run of length n for gray tone i (Assuming the image is Markov)	$\frac{(P_i - P_{ii})^2 (P_{ii})^{n-1}}{P_i^n}$, where $P_i = \sum_j P_{ij}$

Fig. 7. 7 of the common features computed from the cooccurrence probabilities.

where # denotes the number of elements in the set.

Note that these matrices are symmetric; $P(i,j;d,a) = P(j,i;d,a)$. The distance metric ρ implicit in the above equations can be explicitly defined by $\rho((k,l),(m,n)) = \max\{|k-m|, |l-n|\}$.

Consider Fig. 6(a), which represents a 4 × 4 image with four gray tones, ranging from 0 to 3. Fig. 6(b) shows the general form of any gray tone spatial dependence matrix. For example, the element in the (2, 1)th position of the distance 1 horizontal P_H matrix is the total number of times two gray tones of value 2 and 1 occurred horizontally adjacent to each other. To determine this number, we count the number of pairs of resolution cells in R_H such that the first resolution cell of the

pair has gray tone 2 and the second resolution cell of the pair has gray tone 1. In Figs. 6(c) through 6(f), we calculate all four distance 1 gray tone spatial dependence matrices.

Using features calculated from the cooccurrence matrix (see Fig. 7), Haralick *et al.* [28] performed a number of identification experiments. On a set of aerial imagery and eight terrain classes (old residential, new residential, lake, swamp, marsh, urban, railroad yard, scrub, or wooded), an 82 percent correct identification was obtained. On a LANDSAT Monterey Bay, CA, image, an 84 percent correct identification was obtained using 64 X 64 subimages and both spectral and textural features on seven terrain classes: coastal forest, woodlands, annual grasslands, urban areas, large irrigated fields, small irrigated fields, and water. On a set of sandstone photomicrographs, an 89 percent correct identification was obtained on five sandstone classes: Dexter-*L*, Dexter-*H*, St. Peter, Upper Muddy, and Gaskel.

The wide class of images on which they found that spatial gray tone dependence carries much of the texture information is probably indicative of the power and generality of this approach.

The approximate two dozen cooccurrence features times the number of distance angle relationships the cooccurrence matrices can be computed for lead to a potentially large number of dependent features. Tou and Chang [88] discuss an eigenvector-based feature extraction approach to help alleviate this problem.

The experiments of Weszka *et al.* [92] suggest that the spatial frequency features and, therefore, the autocorrelation feature are not as good measures of texture as the cooccurrence features. We suspect that the reason why cooccurrence probabilities have so much more information than the autocorrelation function is that there tends to be natural constraints between the cooccurrence probabilities at one spatial distance with those at another. By these relationships, a lot of information at one spatial distance can determine the smaller amount of information in the autocorrelation function at many spatial distances.

To illustrate this, consider the one-dimensional conditional cooccurrence probabilities $\{p_{ij}(\tau)\}$ for some specific spatial distance τ. Letting μ be the mean gray tone and σ^2 be the gray tone variance, and p_j be the probability of gray tone j occurring, the autocorrelation function can be written in terms of p_{ij} by

$$\rho(\tau) = \frac{\sum_{i,j}(i-\mu)(j-\mu)p_{ij}(\tau)p_j}{\sigma^2}.$$

Hence, for distance 2τ we have

$$\rho(2\tau) = \frac{\sum_{i,j}(i-\mu)(j-\mu)p_{ij}(2\tau)p_j}{\sigma^2}.$$

Assuming the texture is Markov, we have a relationship between $\{p_{ij}(\tau)\}$ and $\{p_{ij}(2\tau)\}$. Namely,

$$p_{ij}(2\tau) = \sum_k p_{ik}(\tau)p_{kj}(\tau).$$

The conditional cooccurrence at one distance can determine the conditional cooccurrence probabilities at another larger distance. Since for any distance, the autocorrelation function is determined by the cooccurrence probabilities, we have that to the extent the texture is Markov, the cooccurrence probabilities at one distance determine the autocorrelation function at many distances.

Because the conditional cooccurrence probabilities are based on a directed distance rather than the undirected distances typically used in the symmetric cooccurrence probabilities, some valuable information may be lost in the symmetric approach. The extent to which such information is lost has not been extensively studied [11].

G. A Textural Transform

We wish to construct an image J such that the gray tone $J(i,j)$ at resolution cell (i,j) in image J indicates how common the texture pattern is in and around resolution cell (i, j) of image I. We call the image J the textural transform of I [25].

For analysis of the microtexture, the gray tone $J(i,j)$ can be a function of the gray tone $I(i,j)$ and its nearest neighbors.

$$J(i,j) = f(I(i-1,j-1), I(i-1,j), I(i-1,j+1), I(i,j-1), \cdot I(i,j), I(i,j+1), I(i+1,j-1), I(i+1,j), \cdot I(i+1,j+1)).$$

Let us assume that this function f is an additive effect of horizontal, right diagonal, vertical, and left diagonal relationships. Then

$$J(i,j) = f_1(I(i,j-1), I(i,j), I(i,j+1)) \quad \text{(horizontal)}$$
$$+ f_2(I(i+1,j-1), I(i,j), I(i-1,j+1)) \quad \text{(right diagonal)}$$
$$+ f_3(I(i-1,j), I(i,j), I(i+1,j)) \quad \text{(vertical)}$$
$$+ f_4(I(i+1,j+1), I(i,j), I(i-1,j-1)) \quad \text{(left diagonal).}$$

But since we do not distinguish between horizontal-left and horizontal-right, or right diagonal up-right and right diagonal down-left, or vertical up and vertical down, or left diagonal up-left and left diagonal down-right, the functions f_1, f_2, f_3, and f_4 have additional symmetries. Assuming the spatial relationships between which we do not distinguish contribute additively, we obtain

$$J(i,j) = h_1(I(i,j), I(i,j-1)) + h_1(I(i,j), I(i,j+1)) \quad \text{(horizontal)}$$
$$+ h_2(I(i,j), I(i+1,j-1)) + h_2(I(i,j), I(i-1,j+1)) \quad \text{(right diagonal)}$$
$$+ h_3(I(i,j), I(i-1,j)) + h_3(I(i,j), I(i+1,j)) \quad \text{(vertical)}$$
$$+ h_4(I(i,j), I(i+1,j+1)) + h_4(I(i,j), I(i-1,j-1)) \quad \text{(left diagonal)}$$

where the functions h_1, h_2, h_3, and h_4 are symmetric functions of two arguments.

Since we want the h functions to indicate relative frequency of the gray-tone spatial pattern, the natural choice is to make each h the cooccurrence probability corresponding to the horizontal, right diagonal, vertical, or left diagonal spatial relationships.

This concept of textural transform can be generalized to any spatial relationship in the following way.

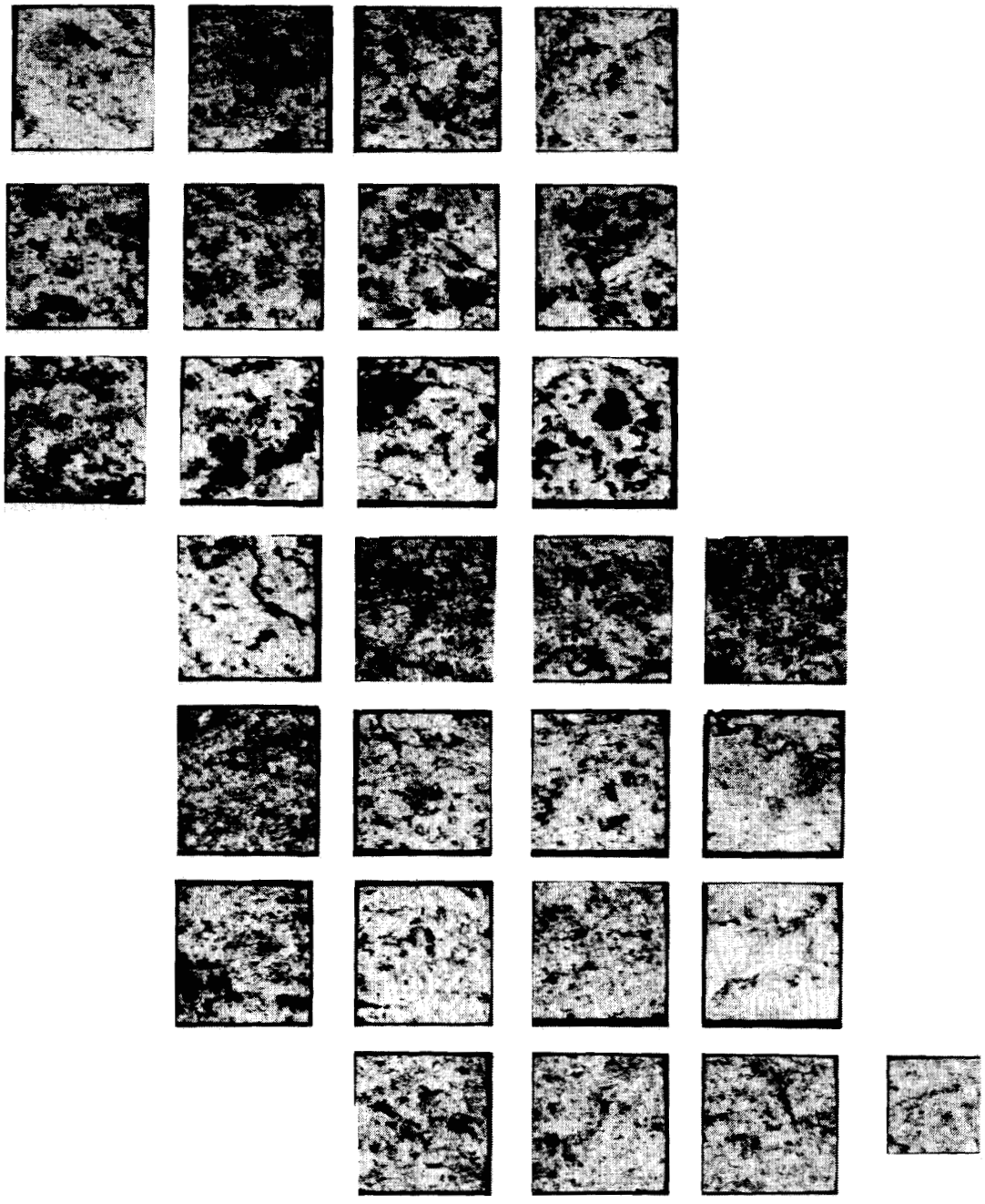

Fig. 8. Subimages in the test area.

Let $Z_r \times Z_c$ be the set of resolution cells of an image I (by row-column coordinates). Let G be the set of gray tones possible to appear on image I. Let R be a binary relation on $Z_r \times Z_c$ pairing together all those resolution cells in the desired spatial relation. The cooccurrence matrix P, $P: G \times G \rightarrow [0, 1]$, for image I and binary relation R is defined by

$$P(i, j) = \frac{\#\{((a, b), (c, d)) \in R \mid I(a, b) = i \text{ and } I(c, d) = j\}}{\#R}.$$

The textural transform J, $J: Z_r \times Z_c \rightarrow (-\infty, \infty)$ of image I relative to function f is defined by

$$J(r, c) = \frac{1}{\#R(r, c)} \sum_{(a, b) \in R(r, c)} f[P(I(r, c), I(a, b))].$$

Assuming f to be the identity function, the meaning of $J(r, c)$ is as follows. The set $R(r, c)$ is the set of all those resolution cells in $Z_r \times Z_c$ in the desired spatial relation to resolution cell (r, c). For any resolution cell $(a, b) \in R(r, c)$, $P(I(r, c), I(a, b))$ is the relative frequency by which the gray tone $I(r, c)$, appearing at resolution cell (r, c), and the gray tone $I(a, b)$, appearing at resolution cell (a, b), cooccur in the desired spatial relation on the entire image. The sum

$$\sum_{(a, b) \in R(r, c)} P(I(r, c), I(a, b))$$

is just the sum of the relative frequencies of gray tone cooccurrence over all resolution cells in the specified relation to resolution (r, c). The factor $1/\#R(r, c)$, the reciprocal of the

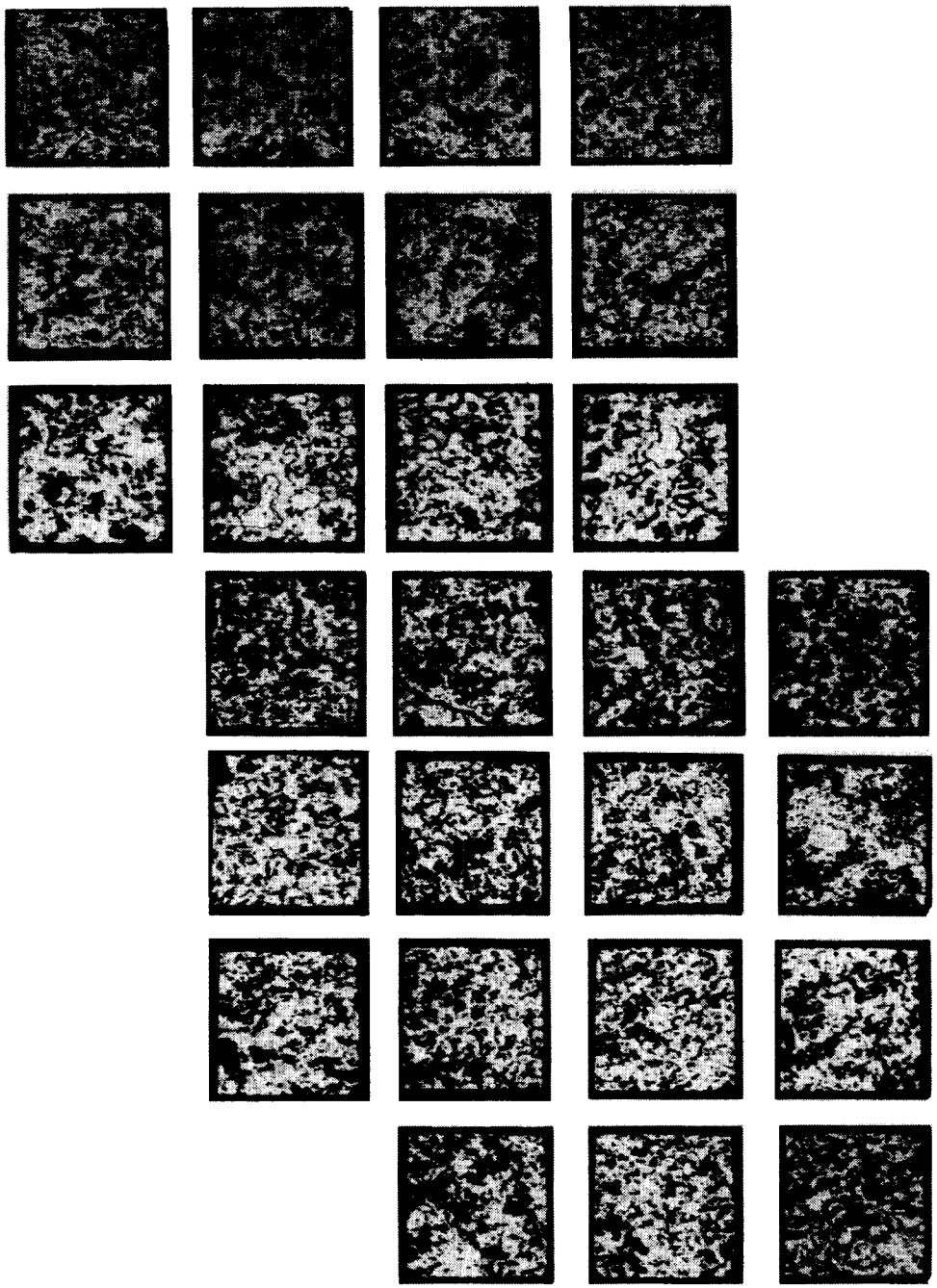

Fig. 9. The textural transforms of the subimages of Fig. 8.

number of resolution cells in the desired spatial relation to (r, c), is just a normalizing factor.

Fig. 8 illustrates 27 100 X 100 subimage of band 5 LANDSAT image 1247-15481 laid out according to their proper relationships in the test area. Fig. 9 illustrates the textural transforms of these subimages also laid out according to their proper relationships in the test area. Gray tones which are white are indicative of frequently occurring textural patterns in the corresponding area on the original subimage. Gray tones which are black are indicative of infrequently occurring textural patterns in the corresponding area on the original image. This means that the same land use type, depending on how frequently it occurs, can be black or white on the textural transform image.

Examining image (0, 0) we notice that Thompson Lake, a *U*-shaped white area on the lower left side of the subimage and a white area on the right side of the subimage have black tones on the transform image. On image (0, 1) Lake Chemung has a large enough area so that its solid black texture appears as a middle gray on the transform image. One image (2, 3) Whitmore Lake has a large enough area so that it appears white on the transform image.

We will take a few enlargements of the subimages and their transforms and interpret the textural transform images in terms of the gray tone spatial dependence patterns. Fig. 10 shows an enlargement of subimage (1, 3) and its transform. Textures consisting of white tones occurring next to white or light gray tones are the most infrequently occurring textural

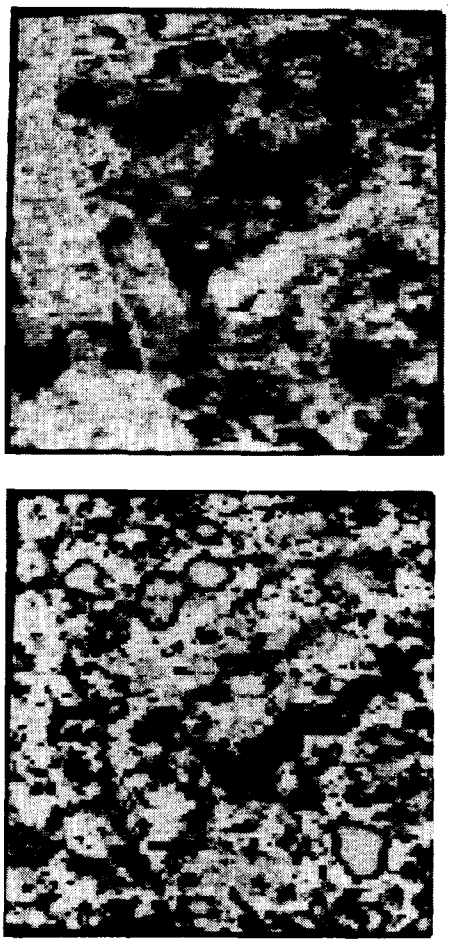

Fig. 10. An enlargement of subimage (1, 3) and its transform.

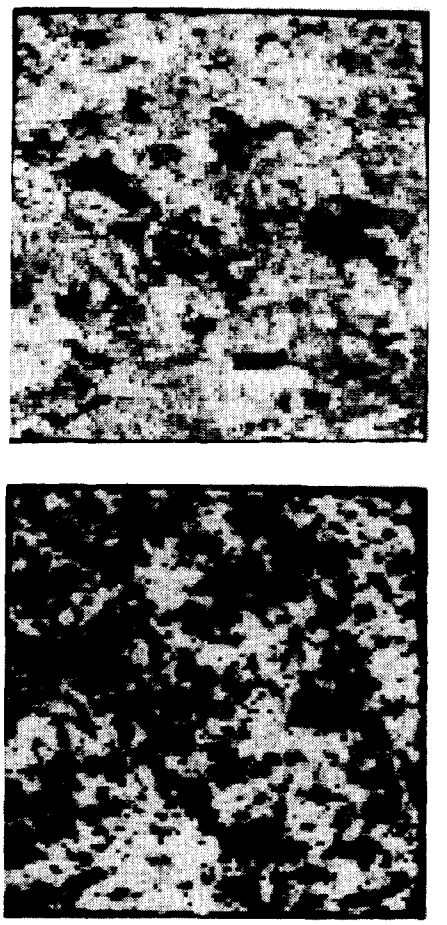

Fig. 11. An enlargement of subimage (6, 0) and its transform.

patterns and they appear as black in the transform image. Finally, Fig. 11 shows an enlargement of subimage (6, 0) where white tones occurring together or black tones occurring together are the most infrequently occurring textural patterns and they appear as black in the transform image.

H. Generalized Gray-Tone Spatial Dependence Models for Texture

Given a specific kind of spatial neighborhood (such as a 3×2 neighborhood or a 5×5 neighborhood) and a subimage, it is possible to compute or estimate the joint probability distribution of the gray tone of the neighborhood in the subimage. In the case of a 5×5 neighborhood, the joint distribution would be 25-dimensional. The generalized gray tone spatial dependence model for texture is based on this joint distribution. Here, the neighborhood is the primitive, the arrangement of its gray tones is the property, and the texture is characterized by the joint distribution of the gray tones in the neighborhood.

Assuming equal prior probabilities, the probability that any neighborhood belongs to texture class k is proportional to the probability of the arrangement of the gray tones in the neighborhood as given by the joint distribution for texture class k. A neighborhood can be assigned to texture class k if the joint distribution for class k is maximal.

The problem with the technique is the high dimensionality for the probability distributions. Parametric representation of the distribution by its first two moments naturally leads to the characterization of texture by the autocorrelation function or power spectrum. Such approaches were discussed in Sections II-B and II-C. Nonparametric representation of the distribution by histogramming the high-dimensional distributions have sample size and storage problems. In the remainder of this section, we review a discrimination technique for representing the nonzero support for these distributions.

Histogram approaches to representing the neighborhood distribution function must pay a heavy storage penalty. For example, a 3×3 neighborhood with 4 quantized values for each gray tone requires 4^9 storage locations (over 250 000). To handle this problem, Read and Jayaramamurthy [67] and McCormick and Jayaramamurthy [53] suggest using the set covering methodology of Michalski [54] and Michalski and McCormick [55] to keep track of those histogram bins which would be nonempty. This technique allows for the generalization of the observed texture samples for each class and provides a simple table look-up sort of decision rule [26].

To see how this works, let the given type of neighborhood contain N resolution cells and let G be the set of quantized gray tones. Then G^N is the set of all possible arrangements of gray tones in the neighborhood. Let $S_k \subseteq G^N$ be the training set of all observed neighborhoods of texture class k, $k = 1, \cdots, K$. We will assume that $S_k \cap S_m = \phi$ for $k \neq m$.

To generalize the training sets, we employ a cylinder operator [27]. Let J be a subset of the indexes from 1 to N; $J \subseteq \{1, \cdots, N\}$. The cylinder operator Ψ_J operates on N-tuples of G^N constraining all components indexed by J to remain fixed to the values they currently hold and letting go free the values

for all components not indexed by J. In this manner, under the $\Psi_{\{2,\cdots,N\}}$ operator, the N-tuple $(x_1, \cdots, x_N)$ becomes $(*, x_2, \cdots, x_N)$ where $*$ means any value. Formally, for any $A \subseteq G^N$, we define the order $\#J$ cylinder operator Ψ_J by:

$$\Psi_J(A) = \{(g_1, \cdots, g_N) \in G^N \mid \text{for some } (a_1, \cdots, a_N) \in A, g_j = a_j \text{ for all } j \in J\}.$$

The cylinder operator is used to generalize the samples of observed texture from each texture class by creating a minimal cover of that class against all other classes. A cover for class k is a collection of subsets of G^N each of which has nonempty intersection with S_k and empty intersection with S_m, $m \neq k$. An order-M cover of S_k against $\bigcup_{\substack{m=1 \\ m \neq k}}^{K} S_m$ is a collection $\mathcal{L}_k^M$ of subsets of G^N, each subset in the collection generalizing an N-tuple in S_k by an order-M or less cylinder operator. $\mathcal{L}_k^M = \{A \subseteq G^N \mid$ for some $(x_1, \ldots, x_N) \in S_k$ and index set J, $\#J \leq M$ $A = \Psi_J(x_1, \ldots, x_N)$ and $A \cap S_m = \phi, m \neq k\}$.

It is clear that when the observed sample sets S_k are disjoint, it is always possible to find a cover of S_k since we can take the order $M = N$ making $\mathcal{L}_k^N$ contain precisely the singleton sets whose members are elements of S_k. Hence, for large enough M, it is always possible to make $\mathcal{L}_k^M$ satisfy:

$$S_k \subseteq \bigcup_{A \in \mathcal{L}_k^M} A \subseteq \left(\bigcup_{\substack{l=1 \\ l \neq k}} S_l \right)^c. \tag{1}$$

We will call an order-M cover minimal if by using cylinder operators only of order less than M equation (1) cannot be satisfied.

The labeling of neighborhoods by texture class can proceed in the following way. Let $\mathcal{L}_1, \ldots, \mathcal{L}_K$ be minimal covers. Let $(g_1, \ldots, g_N)$ be an N-tuple of gray tones from a neighborhood. If the N-tuple is in the cover for class k and for no other class, then assign it to class k. Hence, if:

1) $(g_1, \ldots, g_N) \in \bigcup_{A \in \mathcal{L}_k} A$

2) $(g_1, \ldots, g_N) \notin \bigcup_{A \in \mathcal{L}_m} A, \quad m \neq k$

then we assign the neighborhood to texture class k. If there exists no class so that 1) and 2) are simultaneously satisfied, then we reserve decision.

Using a decision rule similar to this but with a definition for cover minimality which makes the cover dependent on the order in which the N-tuples are encountered, Read and Jayaramamurthy [67] achieved a 78 percent correct identification in distinguishing two textures of chromatin samples and artifact samples from pap smears using a 3 × 2 neighborhood and a 4 gray level quantization.

I. Run Lengths

A gray level run length primitive is a maximal collinear connected set of pixels all having the same gray tone. Gray level runs can be characterized by the gray tone of the run, the length of the run, and the direction of the run. Galloway [21] used 4 directions: 0°, 45°, 90°, and 135°, and for each of these directions she computed the joint probability of gray tone of run and run length.

Let $p(i, j)$ be the number of times there is a run of length j and having gray tone i. Let N_g be the number of gray tones and N_r be the number of runs. Useful statistics of the $p(i, j)$ include:

$$\sum_{i=1}^{N_g} \sum_{j=1}^{N_r} \frac{p(i,j)}{j^2} \Big/ \sum_{i=1}^{N_g} \sum_{j=1}^{N_r} p(i,j) \qquad \text{(short run emphasis inverse moments)}$$

$$\sum_{i=1}^{N_g} \sum_{j=1}^{N_r} j^2 p(i,j) \Big/ \sum_{i=1}^{N_g} \sum_{j=1}^{N_r} p(i,j) \qquad \text{(long run emphasis moments)}$$

$$\sum_{i=1}^{N_g} \left(\sum_{j=1}^{N_r} p(i,j) \right)^2 \Big/ \sum_{i=1}^{N_g} \sum_{j=1}^{N_r} p(i,j) \qquad \text{(gray level nonuniformity)}$$

$$\sum_{j=1}^{N_r} \left(\sum_{i=1}^{N_g} p(i,j) \right)^2 \Big/ \sum_{i=1}^{N_g} \sum_{j=1}^{N_r} p(i,j) \qquad \text{(run length nonuniformity)}$$

$$\sum_{i=1}^{N_g} \sum_{j=1}^{N_r} p(i,j) \Big/ \sum_{i=1}^{N_g} \sum_{j=1}^{N_r} j p(i,j) \qquad \text{(fraction of image in runs).}$$

Using these five measures for each of 4 directions, and one of Haralick's data sets, Galloway illustrated that about 83 percent identification could be made of the six categories: swamp, lake railroad, orchard, scrub, and suburb.

J. Autoregression Models

The linear dependence one pixel of an image has on another is well known and can be illustrated by the autocorrelation function. This linear dependence is exploited by the autoregression model for texture which was first used by McCormick and Jayaramamurthy [52] to synthesize textures. McCormick and Jayaramamurthy used the Box and Jenkins [6] time series seasonal analysis method to estimate the parameters of a given texture. They then used the estimated parameters and a given set of starting values to illustrate that the synthesized texture was close in appearance to the given texture. Deguchi and Morishita [15], Tou *et al.* [89], and Tou and Chang [87] also use a similar technique.

Fig. 12 shows this texture synthesis model. Given a randomly generated noise image and any sequence of K synthesized gray tone values in a scan, the next gray tone value can be synthesized as a linear combination of the previously synthesized values plus a linear combination of previous L random noise values. The coefficients of these linear combinations are the parameters of the model.

Although the one-dimensional model employed by Read and Jayaramamurthy worked reasonably well for the two vertical streaky textures on which they illustrated the technique, performance would be poorer on diagonal wiggly streaky textures. Better performance on general textures would be achieved by a full two-dimensional model illustrated in Fig. 13. Here a pixel (i, j) depends on a two-dimensional neighborhood $N(i, j)$ consisting of pixels above or to the left of it as opposed to the simple sequence of the previous pixels a raster scan could define. For each pixel (k, l) in an order-D neighborhood for pixel (i, j), (k, l) must be previous to pixel (i, j) in a standard raster sequence and (k, l) must not have any coordinates more than D units away from (i, j). Formally, the order-D neighborhood is defined by:

$$N(i,j) = \{(k,l) \mid (i - D \leq k < i \text{ and } j - D \leq l \leq j + D) \text{ or } (k = i \text{ and } j - D \leq l < j)\}.$$

The autoregressive model can be employed in texture segmentation applications as well as texture synthesis applications. Let $\{a_c(m, n), \beta_c(m, n)\}$ be the coefficients for texture category c and let θ be a threshold value. Define the estimated

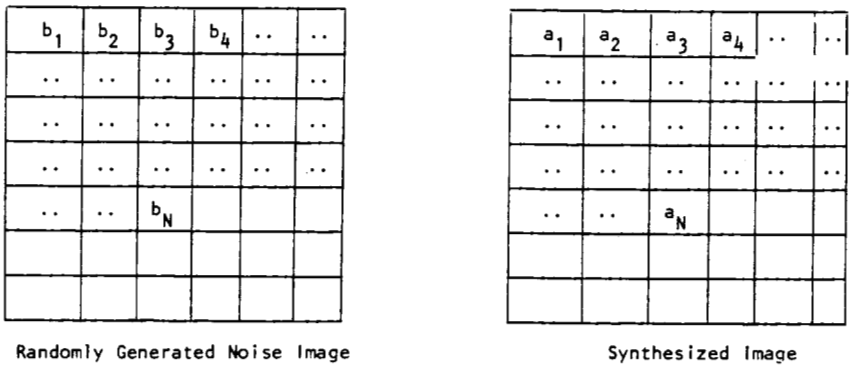

$$a_{N+1} = \underbrace{\sum_{k=0}^{K-1} \alpha_k \, a_{N-k}}_{\text{Auto-Regressive Terms}} + \underbrace{\sum_{\ell=0}^{L-1} \beta_\ell \, b_{N-\ell}}_{\text{Moving Average Terms}}$$

Fig. 12. Illustration of how from a randomly generated noise image and a given starting sequence $a_1, \ldots, a_K$, representing the initial boundary conditions, all values in a texture image can be synthesized by a one-dimensional autoregressive model.

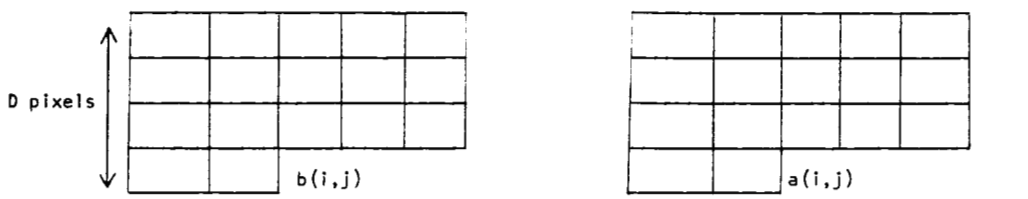

$$a(i,j) = \underbrace{\sum_{(k,\ell)\,\varepsilon\,N(i,j)} \alpha(i-k,\ell-j)\, a(k,\ell)}_{\text{Auto-Regressive Terms}} + \underbrace{\sum_{(k,\ell)\,\varepsilon\,N(i,j)} \beta(i-k,\ell-j)\, b(k,\ell)}_{\text{Moving Average Terms}}$$

Fig. 13. Illustration of how from a randomly generated noise image and a given starting sequence for the first-order D neighborhood in the image, all values in a texture image can be synthesized by a two-dimensional autoregressive model.

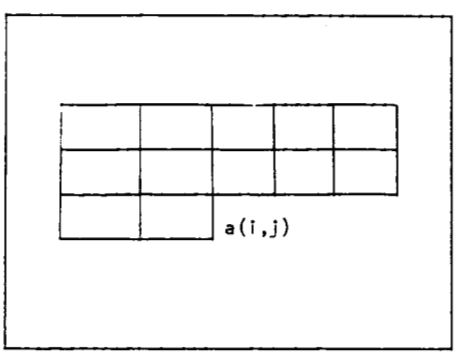

$$\hat{a}(i,j) = \underbrace{\sum_{(k,\ell)\,\varepsilon\,N(i,j)} \alpha(i-k,\ j-\ell)\, a(k,\ell)}_{\text{Auto-Regressive Terms}} + \underbrace{\sum_{(k,\ell)\,\varepsilon\,N(i,j)} \beta(i-k,\ j-\ell)\left[a(k,\ell) - \hat{a}(k,\ell)\right]}_{\text{Moving Average Terms}}$$

Fig. 14. Illustration of how a gray tone value for pixel (i, j) can be estimated using the gray tone values in the neighborhood $N(i, j)$ and the differences between the actual values and the estimated values in the neighborhood.

value of the gray tone at resolution cell (i, j) by:

$$\hat{a}_c(i, j) = \sum_{(k,l)\in N(i,j)} a_c(i-k, j-l)\, a_c(k, l) + \sum_{(k,l)\in N(i,j)} \beta_c(i-k, j-l)\,[a_c(k, l) - \hat{a}_c(k, l)].$$

(See Fig. 14.)

Assuming a uniform prior distribution, we can decide pixel (i, j) has texture category k if:

$$|a(i, j) - \hat{a}_k(i, j)| \leqslant |a(i, j) - \hat{a}_l(i, j)| \text{ for every } l$$

$$\text{and } |a(i, j) - \hat{a}_k(i, j)| \leqslant \theta.$$

if $|a(i, j) - a_k(i, j)| > \theta$, then decide pixel (i, j) is a boundary pixel.

Those readers interested in general two-dimensional estimation procedures for images will find Woods [94] of interest.

K. Mosaic Texture Models

Mosaic texture models tessellate a picture into regions and assign a gray level to the region according to a specified probability density function [100]. Among the kinds of mosaic models are the Occupancy Model [101], the Johnson-Mehl Model [102], the Poisson Line Model [103], and the Bombing Model [104]. The mosaic texture models seem particularly amenable to statistical analysis. It is not known how general these models really are and they are mentioned here for completeness.

III. Structural Approaches to Texture Models

Pure structural models of texture are based on the view that textures are made up of primitives which appear in near regular repetitive spatial arrangements. To describe the texture, we must describe the primitives and the placement rules [73]. The choice of which primitive from a set of primitives and the probability of the chosen primitive being placed at a particular location can be a strong or weak function of location or the primitives near the location.

Carlucci [8] suggests a texture model using primitives of line segments, open polygons, and closed polygons in which the placement rules are given syntactically in a graph-like language. Zucker [98] conceives of real texture as being a distortion of an ideal texture. The underlying ideal texture has a nice representation as a regular graph in which each node is connected to its neighbors in an identical fashion. Each node corresponds to a cell in a tessellation of the plane. The underlying ideal texture is transformed by distorting the primitive at each node to make a realistic texture. Zucker's model is more of a competance based model than a performance model.

Lu and Fu [47] give a tree grammar syntactic approach for texture. They divide a texture up into small square windows (9×9). The spatial structure of the resolution cells in the window is expressed as a tree. The assignment of gray tones to the resolution is given by the rules of a stochastic tree grammar. Finally, special case is given to the placement of windows with respect to another in order to preserve the coherence between windows. Lu and Fu illustrate the power of their technique with both texture synthesis and texture experiments.

In the remainder of this section, we discuss some structural-statistical approaches to texture models. The approach is structural in the sense that primitives are explicitly defined. The approach is statistical in that the spatial interaction, or lack of it, between primitives is measured by probabilities.

We classify textures as being weak textures, or strong textures. Weak textures are those which have weak spatial-interaction between primitives. To distinguish between them it may be sufficient to determine the frequency with which the variety of primitive kinds occur in some local neighborhood. Hence, weak texture measures account for many of the statistical textural features. Strong textures are those which have nonrandom spatial interactions. To distinguish between them it may be sufficient to determine, for each pair of primitives, the frequency with which the primitives cooccur in a specified spatial relationship. Thus our discussion will center on the variety of ways in which primitives can be defined and the ways in which spatial relationships between primitives can be defined.

A. Primitives

A primitive is a connected set of resolution cells characterized by a list of attributes. The simplest primitive is the pixel with its gray tone attribute. Sometimes it is useful to work with primitives which are maximally connected sets of resolution cells having a particular property. An example of such a primitive is a maximally connected set of pixels all having the same gray tone or all having the same edge direction.

Gray tones and local properties are not the only attributes which primitives may have. Other attributes include measures of shape of connected region and homogeneity of its local property. For example, a connected set of resolution cells can be associated with its length or elongation of its shape or the variance of its local property.

Many kinds of primitives can be generated or constructed from image data by one or more applications of neighborhood operators. Included in this class of primitives are: 1) connected components, 2) ascending or descending components, 3) saddle components, 4) relative maxima or minima components, 5) central axis components. Neighborhood operators which compute these kinds of primitives can be found in a variety of papers and will not be discussed here–see [1], [27], [69], [71], [74]-[76], [96].

B. Spatial Relationships

Once the primitives have been constructed, we have available a list of primitives, their center coordinates, and their attributes. We might also have available some topological information about the primitives, such as which are adjacent to which. From this data, we can select a simple spatial relationship such as *adjacency* of primitives or *nearness* of primitives and count how many primitives of each kind occur in the specified spatial relationship.

More complex spatial relationships include closest distance or closest distance within an angular window. In this case, for each kind of primitive situated in the texture, we could lay expanding circles around it and locate the shortest distance between it and every other kind of primitive. In this case our co-occurrence frequency is three-dimensional, two dimensions for primitive kind and one dimension for shortest distance. This can be dimensionally reduced to two dimensions by considering only the shortest distance between each pair of like primitives.

C. Weak Texture Measures

Tsuji and Tomita [91] and Tomita, Yachida, and Tsuji [85] describe a structural approach to weak texture measures. First a scene is segmented into atomic regions based on some tonal property such as constant gray tone. These regions are the

primitives. Associated with each primitive is a list of properties such as size and shape. Then they make a histogram of size property or shape property over all primitives in the scene. If the scene can be decomposed into two or more regions of homogeneous texture, the histogram will be multimodal. If this is the case, each primitive in the scene can be tagged with the mode in the histogram it belongs to. A region growing/cleaning process on the tagged primitives yields the homogeneous textural region segmentation.

If the initial histogram modes overlap too much, a complete segmentation may not result. In this case, the entire process can be repeated with each of the then so far found homogeneous texture region segments. If each of the homogeneous texture regions consists of mixtures of more than one type of primitive, then the procedure may not work at all. In this case, the technique of cooccurrence of primitive properties would have to be used.

Zucker *et al.* [99] used a form of this technique by filtering a scene with a spot detector. Nonmaxima pixels on the filtered scene were thrown out. If a scene has many different homogeneous texture regions, the histogram of the relative max spot detector filtered scene will be multimodal. Tagging the maxima with the modes they belong to and region growing/cleaning thus produced the segmented scene.

The idea of the constant gray-level regions of Tsuji and Tomita or the spots of Zucker *et al.* can be generalized to regions which are peaks, pits, ridges, ravines, hillsides, passes, breaks, flats, and slopes [63], [86]. In fact, the possibilities are numerous enough that investigators doing experiments will have a long working period before understanding will exhaust the possibilities. The next three subsections review in greater detail some specific approaches and suggest some generalizations.

1) Edge Per Unit Area: Rosenfeld and Troy [77] and Rosenfeld and Thurston [76] suggested the amount of edge per unit area for a texture measure. The primitive here is the pixel and its property is the magnitude of its gradient. The gradient can be calculated by any one of the gradient neighborhood operators. For some specified window centered on a given pixel, the distribution of gradient magnitudes can then be determined. The mean of this distribution is the amount of edge per unit area associated with the given pixel. The image in which each pixel's value is edge per unit area is actually a defocused gradient image. Triendl [90] used a defocused Laplacian image. Sutton and Hall [83] used such a measure for the automatic classification of pulmonary disease in chest X-rays.

Ohlander [60] used such a measure to aid him in segmenting textured scenes. Rosenfeld [70] gives an example where the computation of gradient direction on a defocused gradient image is an appropriate feature for the direction of texture gradient. Hsu [38] used a variety of gradient-like measures.

2) Run Lengths: The gray level run lengths primitive in its one-dimensional form is a maximal collinear connected set of pixels all having the same gray level. Properties of the primitive can be length of run, gray level, and angular orientation of run. Statistics of these properties were used by Galloway [21] to distinguish between textures.

In the two-dimensional form, the gray level run length primitive is a maximal connected set of pixels all having the same gray level. These maximal homogeneous sets have properties such as number of pixels, maximum or minimum diameter, gray level, angular orientation of maximum or minimum diameter. Maleson [48] has done some work related to maximal homogeneous sets and weak textures.

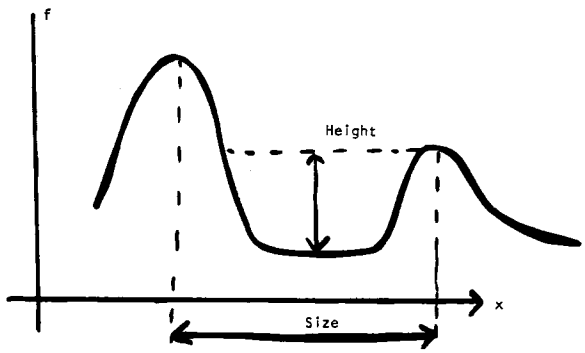

Fig. 15. Illustration of how the height and size properties of a valley are defined.

3) Relative Extrema Density: Rosenfeld and Troy [77] suggest the number of extrema per unit area for a texture measure. They suggest defining extrema in one-dimension only along a horizontal scan in the following way: in any row of pixels, a pixel i is a relative minimum if its gray tone $g(i)$ satisfies:

$$g(i) \leqslant g(i+1) \quad \text{and} \quad g(i) \leqslant g(i-1). \tag{2}$$

A pixel i is a relative maximum if:

$$g(i) \geqslant g(i+1) \quad \text{and} \quad g(i) \geqslant g(i-1). \tag{3}$$

Note that with this definition each pixel in the interior of any constant gray tone run of pixels is considered simultaneously a relative minimum and relative maximum. This is so even if the constant run is just a plateau on the way down or on the way up from a relative extremum.

The algorithm employed by Rosenfeld and Troy marks every pixel in each row which satisfies equations (2) or (3). Then they center a square window around each pixel and count the number of marked pixels. The texture image created this way corresponds to a defocused marked image.

Mitchell, Myers, and Boyne [56] suggest the extrema idea of Rosenfeld and Troy except they proposed to use true extrema and to operate on a smoothed image to eliminate extrema due to noise [7], [18], [19].

One problem with simply counting all extrema in the same extrema plateau as extrema is that extrema per unit area is not sensitive to the difference between a region having few large plateaus of extrema and many single pixel extrema. The solution to this problem is to only count an extrema plateau once. This can be achieved by locating some central pixel in the extrema plateau and marking it as the extrema associated with the plateau. Another way of achieving this is to associate a value of $1/N$ for every extrema in a N-pixel extrema plateau.

In the one-dimensional case, there are two properties that can be associated with every extrema: its height and its width. The height of a maxima can be defined as the difference between the value of the maxima and the highest adjacent minima. The height (depth) of a minima can be defined as the difference between the value of the minima and the lowest adjacent maxima. The width of a maxima is the distance between its two adjacent minima. The width of a minima is the distance between its two adjacent maxima. (Fig. 15 illustrates these properties.)

Two-dimensional extrema are more complicated than one-dimensional extrema. One way of finding extrema in the full

two-dimensional sense is by the iterated use of some recursive neighborhood operators propagating extrema values in an appropriate way. Maximally connected areas of relative extrema may be areas of single pixels or may be plateaus of many pixels. We can mark each pixel in a relative extrema region of size N with the value h indicating that it is part of a relative extrema having height h or mark it with the value h/N indicating its contribution to the relative extrema area. Alternatively, we can mark the most centrally located pixel in the relative extrema region with the value h. Pixels not marked can be given the value 0. Then for any specified window centered on a given pixel, we can add up the values of all pixels in the window. This sum divided by the window size is the average height of extrema in the area. Alternatively we could set h to 1 and the sum would be the number of relative extrema per unit area to be associated with the given pixel.

Going beyond the simple counting of relative extrema, we can associate properties to each relative extrema. For example, given a relative maxima, we can determine the set of all pixels reachable only by the given relative maxima and not by any other relative maxima by monotonically decreasing paths. This set of reachable pixels is a connected region and forms a mountain. Its border pixels may be relative minima or saddle pixels.

The relative height of the mountain is the difference between its relative maxima and the highest of its exterior border pixels. Its size is the number of pixels which constitute it. Its shape can be characterized by features such as elongation, circularity, and symmetric axis. Elongation can be defined as the ratio of the larger to small eigenvalue of the 2×2 second moment matrix obtained from the $\binom{x}{y}$ coordinates of the border pixels [2], [20]. Circularity can be defined as the ratio of the standard deviation to the mean of the radii from the region's center to its border [25]. The symmetric axis feature can be determined by thinning the region down to its skeleton and counting the number of pixels in the skeleton. For regions which are elongated, it may be important to measure the direction of the elongation or the direction of the symmetric axis.

Osman and Saukar [62] use the mean and variance of the height of mountain or depth of valley as properties of primitives. Tsuji and Tomita [91] use size. Histograms and statistics of histograms of these primitive properties are all suitable measures for weak textures.

4) Relational Trees: Ehrich and Foith [18] describe a relational tree representation for the extrema of one-dimensional functions with bounded domains. The relational tree recursively partitions the function and its domain at the smallest relative minimum. The relative minimums for the newly formed segments and functions to the left and right of the dividing point can be used for further divisions. An alternative way to form the tree is to use maximums instead of minimums for dividing.

Fig. 16 illustrates a function and Fig. 17 illustrates its relational tree. The root of the tree indicates that over the entire function domain the highest relative maximum is point 16 and the lowest relative minimum is point 23. The function is then divided at valley 23. The segment to the right of 23 has point 26 for the highest relative maximum and point 27 for the lowest relative minimum, and so on.

Textural features can be extracted at any level of the relational tree. One such texture feature is segment contrast. Segment contrast is the difference between the largest relative maximum and the smallest relative minimum in the segment. The segment contrast textural feature can be the mean or variance of segment contrast taken over the set of segments comprising the given function at a specified level of the tree. Another textural feature can be the variance of segment length.

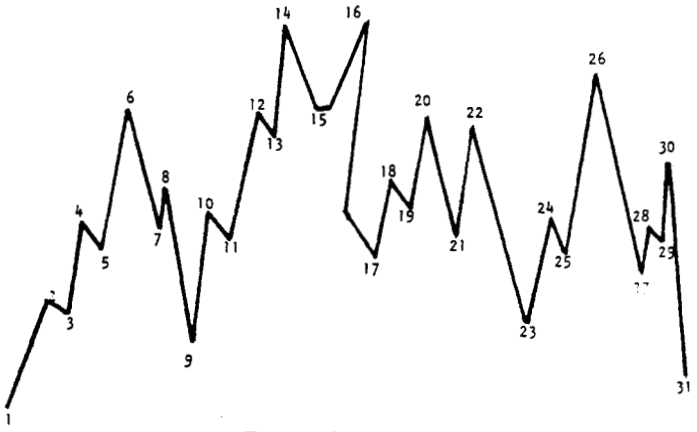

Fig. 16. A waveform.

D. Strong Texture Measures and Generalized Cooccurrence

Strong texture measures take into account the cooccurrence between texture primitives. On the basis of Julesz [40] it is probably the case that the most important interaction between texture primitives occurs as a two-way interaction. Textures with identical second- and lower order interactions but with different higher order interactions tend to be visually similar.

The simplest texture primitive is the pixel with its gray tone property. Gray tone cooccurrence between neighboring pixels was suggested as a measure of texture by a number of researchers as discussed in Section II-F. All the studies mentioned there achieved a reasonable classification accuracy of different textures using cooccurrences of the gray tone primitive.

The next more complicated primitive is a connected set of pixels homogeneous in tone [91]. Such a primitive can be characterized by size, elongation, orientation, and average gray tone. Useful texture measures include cooccurrence of primitives based on relationships of distance or adjacency. Maleson *et al.* [48] suggests using region growing techniques and ellipsoidal approximations to define the homogeneous regions and degree of colinearity as one basis of cooccurrence. For example, for all primitives of elongation greater than a specified threshold, we can use the angular orientation of each primitive with respect to its closest neighboring primitive as a strong measure of texture.

Relative extrema primitives were proposed by Rosenfeld and Troy [77], Mitchell, Myers, and Boyne [56], Ehrich and Foith [18], Mitchell and Carlton [57], and Ehrich and Foith [19]. Cooccurrence between relative extrema was suggested by Davis *et al.* [14]. Because of their invariance under any monotonic gray scale transformation, relative extrema primitives are likely to be very important.

It is possible to segment an image on the basis of relative extrema (for example, relative maxima) in the following way: label all pixels in each maximally connected relative maxima plateau with a unique label. Then label each pixel with the label of the relative maxima that can reach it by a monotonically decreasing path. If more than one relative maxima can reach it by a monotonically decreasing path, then label the

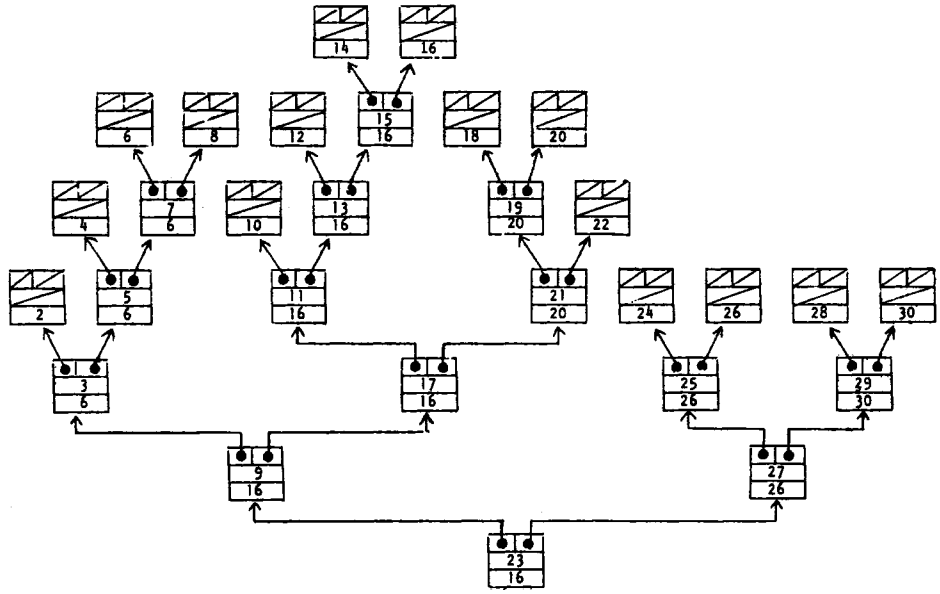

Fig. 17. Ehrich and Foith's relational tree for the waveform of Fig. 16. The first number in each node is the lowest valley point. The second number is the highest peak point for the segment.

pixel with a special label "c" for common. We call the regions so formed the descending components of the image.

Cooccurrence between properties of the descending components can be based on the spatial relationship of adjacency. For example, if the property is size, the cooccurrence matrix could tell us how often a descending component of size s_1 occurs adjacent to or nearby to a descending component of size s_2 or of label "c."

To define the concept of generalized cooccurrence, it is necessary to first decompose an image into its primitives. Let Q be the set of all primitives on the image. Then we need to measure primitive properties such as mean gray tone, variance of gray tones, region, size, shape, etc. Let T be the set of primitive properties and f be a function assigning to each primitive in Q a property of T. Finally, we need to specify a spatial relation between primitives such as distance or adjacency. Let $S \subseteq Q \times Q$ be the binary relation pairing all primitives which satisfy the spatial relation. The generalized cooccurrence matrix P is defined by:

$$P(t_1, t_2) = \frac{\#\{(q_1, q_2) \in S \mid f(q_1) = t_1 \text{ and } f(q_2) = t_2\}}{\#S}.$$

$P(t_1, t_2)$ is just the relative frequency with which two primitives occur with specified spatial relationship in the image, one primitive having property t_1 and the other primitive having property t_2.

Zucker [97] suggests that some textures may be characterized by the frequency distribution of the number of primitives any primitive has related to it. This probability $p(k)$ is defined by:

$$p(k) = \frac{\#\{(q \in Q \mid \#S(q) = k\}}{\#Q}.$$

Although this distribution is simpler than cooccurrence, no investigator appears to have used it in texture discrimination experiments.

Conclusion

We have surveyed the image processing literature on the various approaches and models investigators have used for textures. For microtextures, the statistical approach seems to work well. The statistical approaches have included autocorrelation functions, optical transforms, digital transforms, textural edgeness, structural element, gray tone cooccurrence, and autoregressive models. Pure structural approaches based on more complex primitives than gray tone seems not to be widely used. For macrotextures, investigators seem to be moving in the direction of using histograms of primitive properties and cooccurrence of primitive properties in a structural-statistical generalization of the pure structural and statistical approaches.

Acknowledgment

The help of Lynn Ertebati, who typed the manuscript, is greatly appreciated.

References

[1] C. Arcelli and G. Sanniti Di Baja, "On the sequential approach to medial line transformation," *IEEE Trans. Syst., Man, Cybern.*, vol. SMC-8, pp. 139-144, (Feb. 1978).

[2] R. Bachi, "Geostatistical analysis of territories," presented at *Proc. 39th Session–Bulletin of the Int. Statistical Inst.* (Vienna, Austria, 1973).

[3] R. Bajcsy and L. Lieberman, "Computer description of real outdoor scenes," in *Proc. Second Int. Joint Conf. on Pattern Recognition* (Copenhagen, Denmark), pp. 174-179, Aug. 1974.

[4] —, "Texture gradient as a depth cue," *Comput. Graph. Image Processing*, vol. 5, no. 1, pp. 52-67, 1976.

[5] P. Bartels, G. Bahr, and G. Weid, "Cell recognition from line scan transition probability profiles," *Acta Cytol.*, vol. 13, pp. 210-217, 1969.

[6] J. E. Box and G. M. Jenkins, *Time Series Analysis.* San Francisco, CA: Holden-Day, 1970.

[7] S. G. Carlton and O. Mitchell, "Image segmentation using texture and grey level," in *Pattern Recognition and Image Processing Conf.* (Troy, NY), pp. 387-391, June 1977.

[8] L. Carlucci, "A formal system for texture languages," in *Pattern Recognition*, vol. 4, pp. 53-72, 1972.

[9] P. Chen and T. Pavlidis, "Segmentation by texture using a co-occurrence matrix and a split-and-merge algorithm," Tech. Rep.

237, Princeton University, Princeton, NJ, Jan. 1978.
[10] Y. P. Chien and K. S. Fu, "Recognition of X-ray picture patterns," *IEEE Trans. Syst., Man, Cybern.*, vol. SMC-4, pp. 145–156, Mar. 1974.
[11] R. W. Conners and C. A. Harlow, "Some theoretical considerations concerning texture analysis of radiographic images," presented at *Proc. 1976 IEEE Conf. on Decision and Control*, 1976.
[12] L. J. Cutrona, E. N. Leith, C. J. Palermo, and L. J. Porcello, "Optical data processing and filtering systems," *IRE Trans. Inform. Theory*, vol. 15, no. 6, pp. 386–400, June 1969.
[13] E. M. Darling and R. D. Joseph, "Pattern recognition from satellite altitudes," *IEEE Trans. Syst., Man, Cybern.*, vol. SMC-4, pp. 38–47, Mar. 1968.
[14] L. Davis, S. Johns, and J. K. Aggarwal, "Texture analysis using generalized co-occurrence matrices," presented at *Pattern Recognition and Image Processing Conf.* (Chicago, IL), May 31–June 2, 1978.
[15] K. Deguchi and I. Morishita, "Texture characterization and texture-based image partitioning using two-dimensional linear estimation techniques," presented at *U.S.-Japan Cooperative Science Program Seminar on Image Processing in Remote Sensing* (Washington, DC), Nov. 1–5, 1976.
[16] C. Dyer and A. Rosenfeld, "Courier texture features: suppression of aperature effects," *IEEE Trans. Syst., Man, Cybern.*, vol. SMC-6, pp. 703–705, Oct. 1976.
[17] D. Egbert, J. McCauley, and J. McNaughton, "Ground pattern analysis in the Great Plains," Semi-Annual ERTS A Investigation Rep., Remote Sensing Laboratory, University of Kansas, Lawrence, KS, Aug. 1973.
[18] Roger Ehrich and J. P. Foith, "Representation of random waveforms by relational trees," *IEEE Trans. Comput.*, vol. C-25, pp. 725–736, July 1976.
[19] ——, "Topology and semantics of intensity arrays," *Computer Vision*, Hanson and Riseman (Eds). New York: Academic Press, 1978.
[20] Y. S. Frolov, "Measuring the shape of geographical phenomena: A history of the issue," *Sov. Geog.: Rev. Transla.*, vol. XVI, no. 10, pp. 676–687, Dec. 1975.
[21] M. Galloway, "Texture analysis using gray level run lengths," *Comput. Graphics Image Processing*, vol. 4, pp. 172–199, 1974.
[22] J. W. Goodman, *Introduction to Fourier Optics*. New York: McGraw-Hill Book Co., 1968.
[23] N. Gramenopoulos, "Terrain type recognition using ERTS-1 MSS images," in *Rec. Symp. Significant Results Obtained from the Earth Res. Technol. Satellite*, NASA SP-327, pp. 1229–1241, Mar. 1973.
[24] R. M. Haralick, "A texture-context feature extraction algorithm for remotely sensed imagery," in *Proc. 1971 IEEE Decision and Control Conf.* (Gainesville, FL), pp. 650–657, Dec. 15–17, 1971.
[25] ——, "A textural transform for images," *Proc. IEEE Conf. Computer Graphics, Pattern Recognition, and Data Structure* (Beverly Hills, CA), May 14–15, 1975.
[26] ——, "The table look-up rule," *Commun. Statist.—Theory and Methods*, vol. A5, no. 12, pp. 1163–1191, 1976.
[27] ——, "Structural pattern recognition, homomorphisms, and arrangements," in *Pattern Recognition*, vol. 10, no. 3, June 1978.
[28] R. M. Haralick and R. Bosley, "Texture features for image classification," *Third ERTS Symp.*, NASA SP-351, NASA Goddard Space Flight Center, Greenbelt, MD, pp. 1929–1969, Dec. 10–15, 1973.
[29] R. M. Haralick and K. Shanmugam, "Combined spectral and spatial processing of ERTS imagery data," in *Proc. 2nd Symp. Significant Results Obtained from Earth Resources Technology Satellite-1*, NASA SP-327, NASA Goddard Space Flight Center, Greenbelt, MD, pp. 1219–1228, March 5–9, 1973.
[30] ——, "Computer classification of reservoir sandstones," *IEEE Trans. Geosci. Electron.*, vol. GE-11, pp. 171–177, Oct. 1973.
[31] ——, "Combined spectral and spatial processing of ERTS imagery data," *J. of Remote Sensing of the Environment*, vol. 3, 1974, pp. 3–13.
[32] R. M. Haralick, K. Shanmugam, and I. Dinstein, "On some quickly computable features for texture," *Proc. 1972 Symp. on Comput. Image Processing and Recognition* (University of Missouri, Columbia, MO), vol. 2, pp. 12-2-1 to 12-2-10, Aug. 1972.
[33] ——, "Textural features for image classification," *IEEE Trans. Syst., Man, Cybern.*, vol. SMC-3, pp. 610–621, Nov. 1973.
[34] R. M. Haralick, "Neighborhood operators," unpublished manuscript.
[35] E. E. Hardy and J. R. Anderson, "A land use classification system for use with remote-sensor data," in *Machine Processing of Remotely Sensed Data*. Lafayette, IN, Oct. 1973.
[36] J. K. Hawkins, "Textural properties for pattern recognition," *Picture Processing and Psychopictorics*, Bernic Sacks Lipkin and Azriel Rosenfeld (EDS). New York: Academic Press, 1969.
[37] R. J. Horning and J. A. Smith, "Application of Fourier analysis to multispectral/spatial recognition," presented at Management and Utilization of Remote Sensing Data ASP Symposium, Sioux Falls, SD, Oct. 1973.
[38] S. Hsu, "A texture-tone analysis for automated landuse mapping with panchromatic images," in *Proc. of the Amer. Society for Photogrammetry*, pp. 203–215, Mar. 1977.
[39] B. Julesz, "Visual pattern discrimination," *IRE Trans. Inform. Theory*, vol. 8, no. 2, pp. 84–92, Feb. 1962.
[40] ——, "Experiments in the visual perception of texture," Apr. 1975, 10 pp.
[41] H. Kaizer, "A quantification of textures on aerial photographs," Boston University Research Laboratories, Boston University, Boston, MA, Tech. Note 121, 1955, AD 69484.
[42] L. Kirvida, "Texture measurements for the automatic classification of imagery," *IEEE Trans. Electromagnet. Compat.*, vol. 18, pp. 38–42, Feb. 1976.
[43] L. Kirvida and G. Johnson, "Automatic interpretation of ERTS data for forest management," *Symp. on Significant Results Obtained from the Earth Res. Technol. Satellite*, NASA SP-327, Mar. 1973.
[44] C. Lantuejoul, "Grain dependence test in a polycristalline ceramic," in *Quantitative Analysis of Microstructures in Materials Science, Biology, and Medicine*, J. L. Chernant, Ed. Stuttgart, Germany: Riederer-Verlag, GmbH, 1978, pp. 40–50.
[45] G. Lendaris and G. Stanley, "Diffraction pattern sampling for automatic pattern recognition," *SPIE Pattern Recognition Studies Seminar Proc.* (June 9–10, 1969, pp. 127–154).
[46] ——, "Diffraction pattern samplings for automatic pattern recognition," *Proc. IEEE*, vol. 58, pp. 198–216, Feb. 1970.
[47] S. Y. Lu and K. S. Fu, "A syntactic approach to texture analysis," *Comput. Graph. Image Processing*, vol. 7, pp. 303–330, 1978.
[48] J. Maleson, C. Brown, and J. Feldman, "Understanding natural texture," Computer Science Department, University of Rochester, Rochester, NY, Sept. 1977.
[49] G. Matheron, *Elements Pour Une Theorie des Milieux Poreux*. Paris, France: Masson, 1967.
[50] ——, *Random Sets and Integral Geometry*. New York: Wiley and Sons, Inc., 1975.
[51] H. Maurer, "Texture analysis with Fourier series," *Proc. Ninth Int. Symp. on Remote Sensing of Environment* (Environmental Research Institute of Michigan, Ann Arbor, MI), pp. 1411–1420, Apr. 1974.
[52] B. H. McCormick and S. N. Jayaramamurthy, "Time series model for texture synthesis," *Int. J. Comput. Inform. Sci.*, vol. 3, no. 4, pp. 329–343, Dec. 1974.
[53] ——, "A decision theory method for the analysis of texture," *Int. J. of Comput. Inform. Sci.*, vol. 4, no. 1, pp. 1–38, Mar. 1975.
[54] R. S. Michalski, "On the quasi-minimal solution of the general covering problem," in *Proc. Fifth Int. Symp. on Inform. Processing* (Yugoslavia, Bled), Oct. 1969).
[55] R. S. Michalski and B. H. McCormick, "Interval generalization of switching theory," in *Proc. Third Annu. Houston Conf. on Comput. Syst. Sci.* (Houston, TX), pp. 213–226, Apr. 1971.
[56] Owen Mitchell, Charles Myers, and William Boyne, "A max-min measure for image texture analysis," *IEEE Trans. Comput.*, vol. C-25, pp. 408–414, Apr. 1977.
[57] O. R. Mitchell and S. G. Carlton, "Image segmentation using a local extrema texture measure," Special Issue of *Pattern Recognition*, June 1977.
[58] W. Müller, "The Leitz texture analyzes systems," *Leitz Sci. Tech. Inform.*, Supplement 1, 4, pp. 101–116, Apr. 1974 (Wetzlar, Germany).
[59] W. Müller and W. Herman, "Texture analyzes systems," *Indust. Res.*, Nov. 1974.
[60] R. Ohlander, "Analysis of natural scenes," Ph.D. dissertation, Carnegie-Mellon University, Pittsburgh, PA, 1975.
[61] E. O'Neill, "Spatial filtering in optics," *IRE Trans. Inform. Theory*, vol. 2, no. 6, pp. 56–65, June 1956.
[62] M. O. M. Osman and T. S. Saukar, "The measurement of surface texture by means of random function excursion techniques," in *Advances in Test Measurement*, vol. 12—*Proc. 21st Int. Instrument. Symp.* Pittsburgh, PA: Instrument Society of America, 1975.
[63] T. Peucker and D. Douglas, "Detection of surface-specific points by local parallel processing of discrete terrain elevation data," *Comput. Graph. Image Processing*, vol. 4, no. 4, pp. 375–387, Dec. 1975.

[64] R. M. Pickett, "Visual analyses of texture in the detection and recognition of objects," in *Picture Processing and Psychopictorics*, Lipkin and Rosenfeld, Eds. New York: Academic Press, 1970, pp. 289-308.
[65] N. J. Pressman, "Markovian analysis of cervical cell images," *J. Histochem. Cytochem.*, vol. 24, no. 1, pp. 138-144, 1976.
[66] K. Preston, *Coherent Optical Computers*. New York: McGraw-Hill Book Company, 1972.
[67] J. S. Read and S. N. Jayaramamurthy, "Automatic generation of texture feature detectors," *IEEE Trans. Comput.*, vol. C-21, pp. 803-812, July 1972.
[68] A. Rosenfeld, "Automatic recognition of basic terrain types on aerial photographs," *Photogrammet. Eng.*, vol. 28, pp. 115-132, 1962.
[69] —, "Connectivity in digital pictures," *J. Ass. Comput. Mach.*, vol. 17, no. 1, pp. 146-160, Jan. 1970.
[70] —, "A note on automatic detection of texture gradients," in *IEEE Trans. Comput.*, vol. C-23, pp. 988-991, Oct. 1975.
[71] A. Rosenfeld and L. Davis, "A note on thinning," *IEEE Trans. Syst., Man, Cybern.*, vol. SMC-6, pp. 226-228, Mar. 1976.
[72] A. Rosenfeld and A. Goldstein, "Optical correlation for terrain type discrimination," *Photogrammet. Eng.*, vol. 30, pp. 639-646, 1964.
[73] A. Rosenfeld and B. S. Lipkin, "Texture synthesis," in *Picture Processing and Psychopictorics*, Lipkin and Rosenfeld (Eds). New York: Academic Press, 1970, pp. 309-345.
[74] A. Rosenfeld and J. Pfaltz, "Sequential operations in digital picture processing," *J. Ass. Comput. Mach.*, vol. 13, no. 4, pp. 471-494, Oct. 1966.
[75] A. Rosenfeld and J. Pfaltz, "Distance functions on digital images," *Pattern Recognition*, vol. 1, no. 1, pp. 33-61, 1968.
[76] A. Rosenfeld and M. Thurston, "Edge and curve detection for visual scene analysis," *IEEE Trans. Comput.*, vol. C-20, pp. 562-569, May 1971.
[77] A. Rosenfeld and E. Troy, "Visual texture analysis," Tech. Rep. 70-116, University of Maryland, College Park, MD, June 1970. Also in *Conference Record for Symposium on Feature Extraction and Selection in Pattern Recognition*, Argonne, IL, IEEE Publication 70C-51C, Oct. 1970, pp. 115-124.
[78] J. Serra, "Theoretical bases of the Leitz texture analyses system," *Leitz Sci. Tech. Inform.*, Supplement 1, 4, pp. 125-136, Apr. 1974 (Wetzlar, Germany).
[79] —, "One, two, three, . . . , infinity," *Quantitative Analysis of Microstructures in Materials Science, Biology, and Medicine*, J. L. Chernant (Ed.). Stuttgart, Germany: Riederer-Verlag GmbH, 1978, pp. 9-24.
[80] J. Serra and G. Verchery, "Mathematical morphology applied to fibre composite materials," *Film Sci. Tech.*, vol. 6, pp. 141-158, 1973.
[81] A. R. Shulman, *Optical Data Processing*. New York: Wiley, 1970.
[82] R. Stefanelli and A. Rosenfeld, "Some parallel thinning algorithms for digital pictures," *J. Ass. Comput. Mach.*, vol. 18, no. 2, pp. 255-264, Apr. 1971.
[83] R. Sutton and E. Hall, "Texture measures for automatic classification of pulmonary disease," *IEEE Trans. Comput.*, vol. C-21, no. 1, pp. 667-676, 1972.
[84] G. Swanlund, "Honeywell's automatic tree species classifier," Honeywell Systems and Research Division, Rep. 9D-G-24, Dec. 31, 1969.
[85] F. Tomita, M. Yachida, and S. Tsuji, "Detection of homogeneous regions by structural analysis," at *Proc. Third Int. Joint Conf. Artificial Intelligence*, pp. 564-571, 1973.
[86] J. Toriwaki and T. Fukumura, "Extraction of structural information from grey pictures," *Comput. Graph. Image Processing*, vol. 7, no. 1, pp. 30-51, 1978.
[87] J. T. Tou and Y. S. Chang, "An approach to texture pattern analysis and recognition," in *Proc. 1976 IEEE Conf. on Decision and Control*, 1976.
[88] —, "Picture understanding by machine via textural feature extraction," in *Proc. 1977 IEEE Conf. on Pattern Recognition and Image Processing* (Troy, New York), June 1977.
[89] J. T. Tou, D. B. Kao, and Y. S. Chang, "Pictorial texture analysis and synthesis," presented at *Third Int. Joint Conf. on Pattern Recognition* (Coronado, CA), Aug. 1976.
[90] E. E. Triendl, "Automatic terrain mapping by texture recognition," in *Proceedings of the Eighth International Symposium on Remote Sensing of Environment*. Ann Arbor, MI: Environmental Research Institute of Michigan, Oct. 1972.
[91] S. Tsuji and F. Tomita, "A structural analyzer for a class of textures," *Comput. Graph. Image Processing*, vol. 2, pp. 216-231, 1973.
[92] J. Weszka, C. Dyer, and A. Rosenfeld, "A comparative study of texture measures for terrain classification," *IEEE Trans. Syst., Man, and Cybern.*, vol. SMC-6, no. 4, pp. 269-285, Apr. 1976.
[93] G. Wied, G. Bahr, and P. Bartels, "Automatic analysis of cell images," in *Automated Cell Identification and Cell Sorting*, Wied and Bahr Eds. New York: Academic Press, 1970, pp. 195-360.
[94] J. W. Woods, "Two-dimensional discrete Markovian fields," *IEEE Trans. Inform. Theory*, vol. IT-18, pp. 232-240, Mar. 1972.
[95] A. M. Yaglom, *Theory of Stationary Random Functions*. Englewood Cliffs, NJ: Prentice-Hall, 1962.
[96] S. Yokoi, J. Toriwaki, and T. Fukumura, "An analysis of topological properties of digitized binary pictures using local features," *Comput. Graph. Image Processing*, vol. 4, pp. 63-73, 1975.
[97] S. Zucker, *On the Foundations of Texture: A Transformational Approach*, Tech. Rep. TR-331, University of Maryland, College Park, MD, Sept. 1974.
[98] —, "Toward a model of texture," *Comput. Graph. Image Processing*, vol. 5, no. 2, pp. 190-202, 1976.
[99] S. W. Zucker, A. Rosenfeld, and L. Davis, "Picture segmentation by texture discrimination," *IEEE Trans. Comput.*, vol. C-24, no. 12, pp. 1228-1233, Dec. 1975.
[100] B. J. Schachter, A. Rosenfeld, and L. S. Davis, "Random mosaic models for textures," *IEEE Trans. Syst., Man, Cybern.*, vol. SMC-8, no. 9, pp. 694-702, Sept. 1978.
[101] R. Miles, "On the homogeneous planar Poisson point-process," *Math. Biosci.*, vol. 6, pp. 85-127, 1970.
[102] E. Gilbert, "Random subdivisions of space into crystals," *Annals Math. Stat.*, vol. 33, pp. 958-972, 1962.
[103] R. Miles, "Random polygons determined by random lines in the plane," *Proc. Nat. Acad. Sci. USA*, vol. 52, pp. 901-907, pp. 1157-1160.
[104] P. Switzer, "Reconstructing patterns for sample data," *Annals Math. Stat.*, vol. 38, pp. 138-154, 1967.

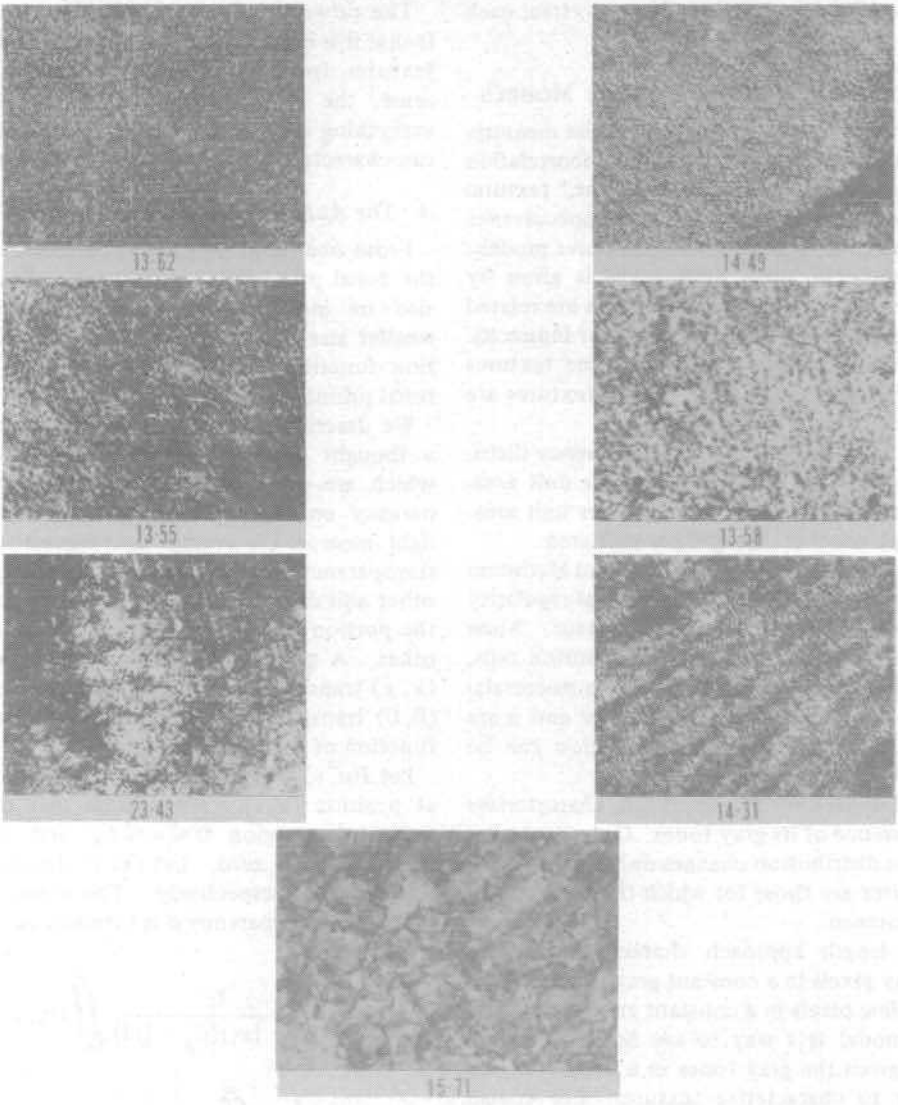

Fig. 1. Some of the image textures used by Kaizer in his autocorrelation experiment [41].

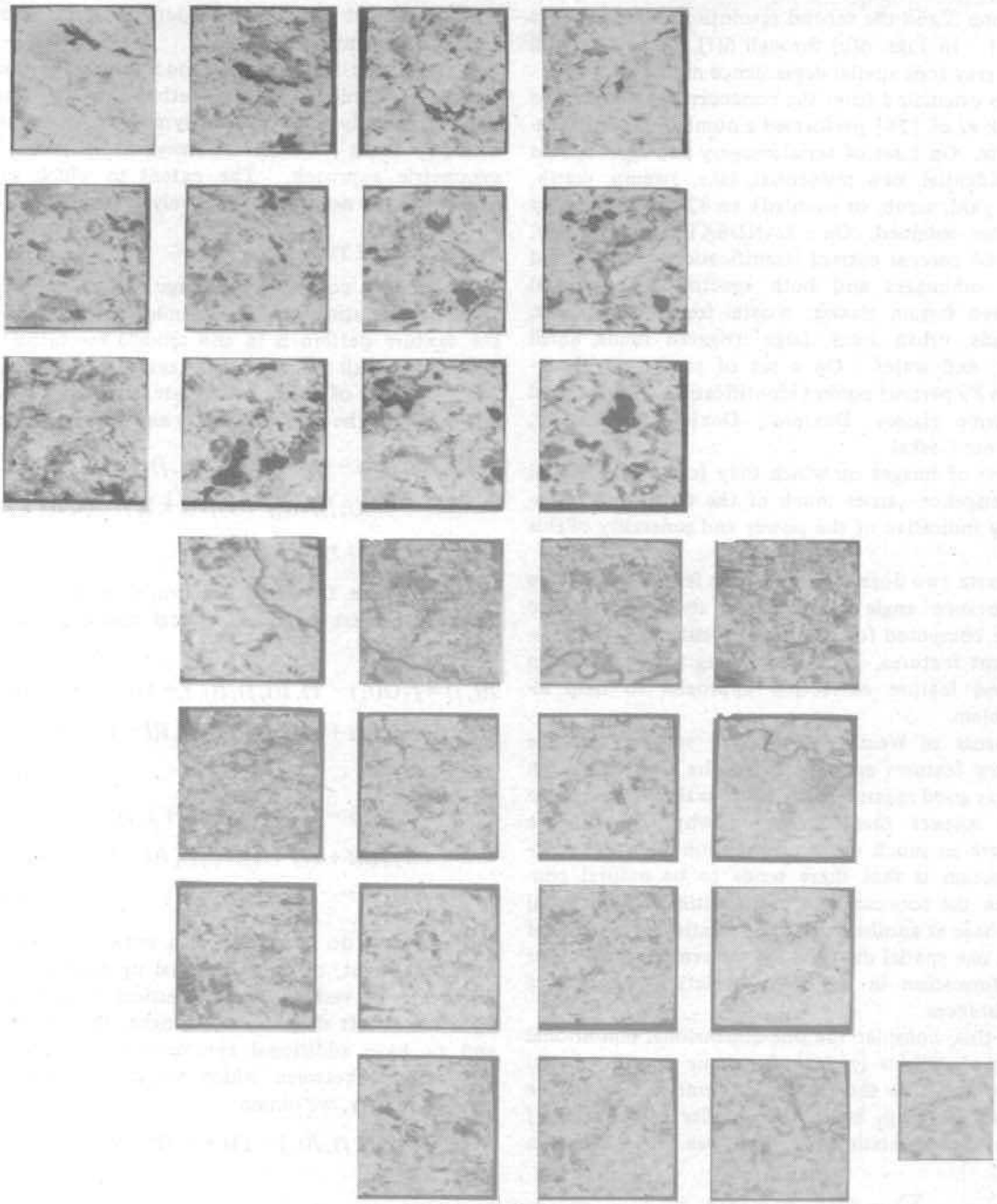

Fig. 8. Subimages in the test area.

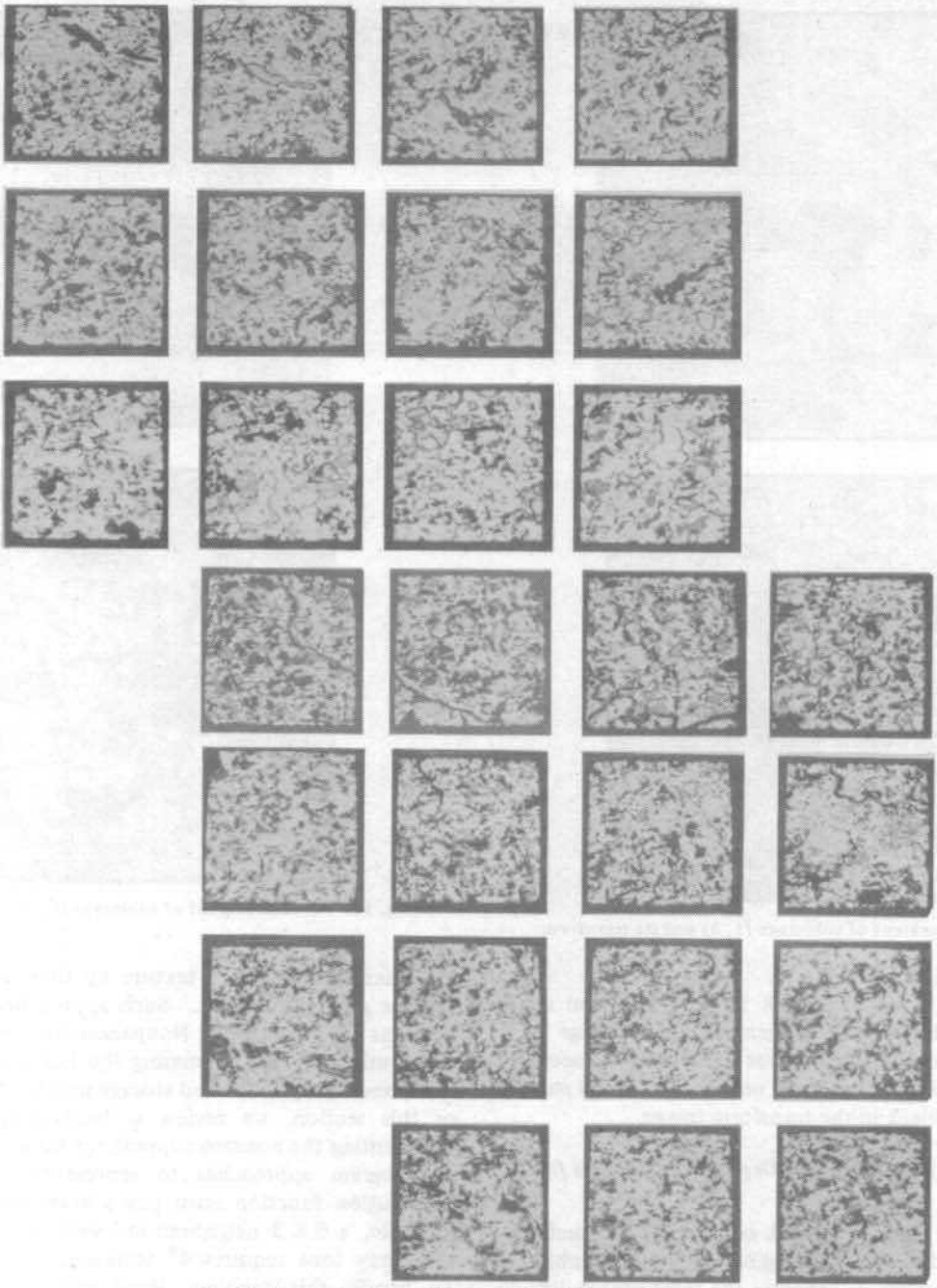

Fig. 9. The textural transforms of the subimages of Fig. 8.

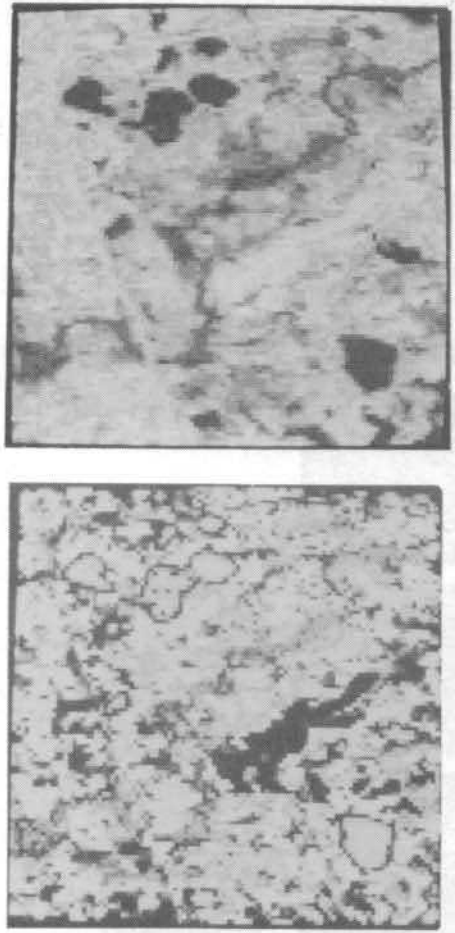

Fig. 10. An enlargement of subimage (1, 3) and its transform.

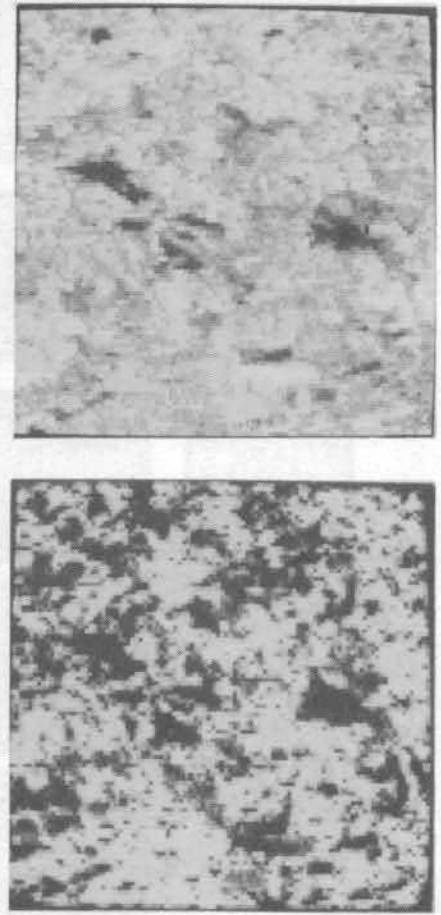

Fig. 11. An enlargement of subimage (6, 0) and its transform.